iScience

CellPress
OPEN ACCESS

Article

A moderate dosage of prostaglandin E2-mediated annexin A1 upregulation promotes alkali-burned corneal repair

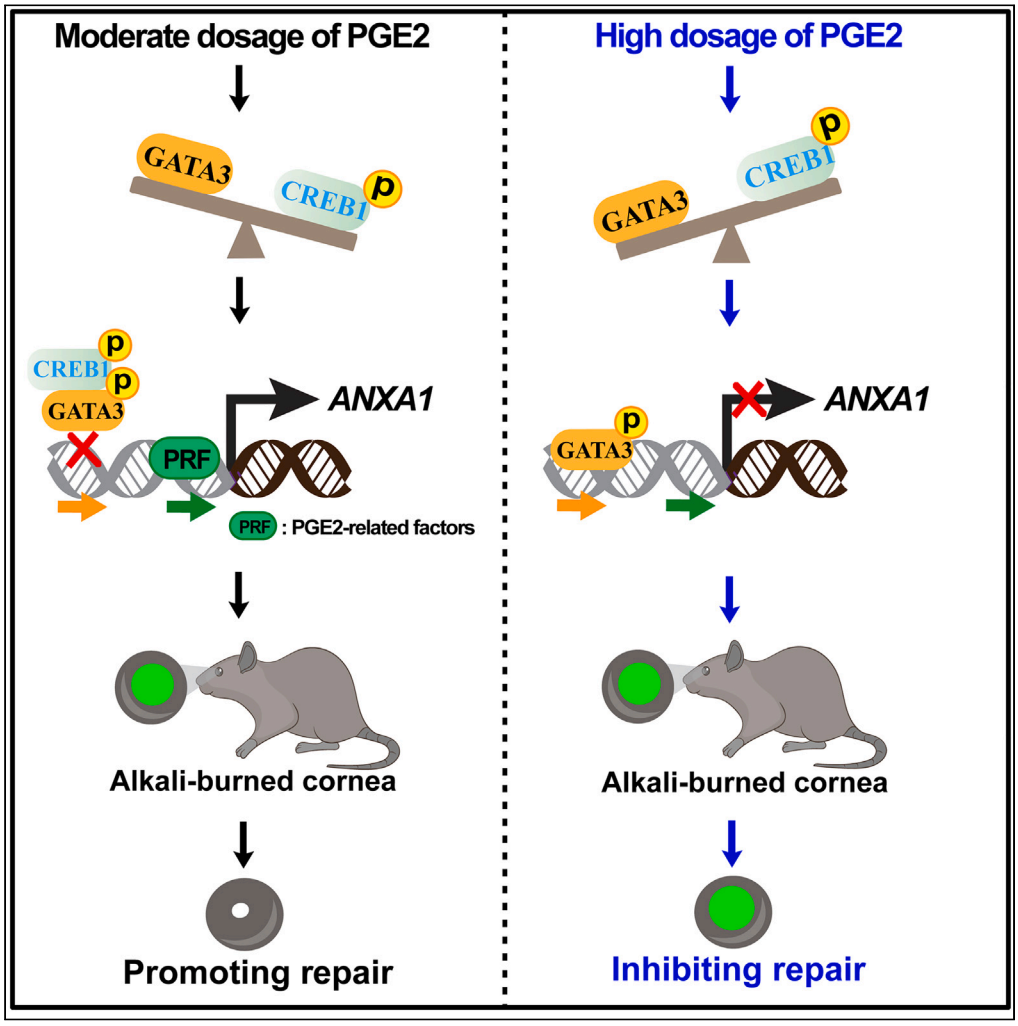

Hongling Liu, Xue Zhang, Qiang Tan, ..., Baishijiao Bian, Yijian Li, Yong Liu

ccleqq@aliyun.com (B.B.)
Liyijian2226@163.com (Y.L.)
liuyy99@163.com (Y.L.)

Highlights

A moderate dosage of PGE2 increases ANXA1 to accelerate alkali-burned corneal repair

A high dosage of PGE2 reduces ANXA1 to postpone alkali-burned corneal repair

A high dosage of PGE2 downregulates ANXA1 by enhancing GATA3 binding to its promoter

A moderate dosage of PGE2 induces higher GATA3 and lower CREB1 phosphorylation

Liu et al., iScience *26*, 108565
December 15, 2023
https://doi.org/10.1016/j.isci.2023.108565

iScience

CellPress
OPEN ACCESS

Article

A moderate dosage of prostaglandin E2-mediated annexin A1 upregulation promotes alkali-burned corneal repair

Hongling Liu,[1,2,6] Xue Zhang,[1,2,6] Qiang Tan,[1,2] Lingling Ge,[1,2] Jia Lu,[1,2] Chunge Ren,[1,2] Baishijiao Bian,[1,2,3,4,*] Yijian Li,[1,2,*] and Yong Liu[1,2,5,7,*]

SUMMARY

Corneal alkali burn remains a clinical challenge in ocular emergency, necessitating the development of effective therapeutic drugs. Here, we observed the arachidonic acid metabolic disorders of corneas induced by alkali burns and aimed to explore the role of Prostaglandin E2 (PGE2), a critical metabolite of arachidonic acid, in the repair of alkali-burned corneas. We found a moderate dosage of PGE2 promoted the alkali-burned corneal epithelial repair, whereas a high dosage of PGE2 exhibited a contrary effect. This divergent effect is attributed to different dosages of PGE2 regulating ANXA1 expression differently. Mechanically, a high dosage of PGE2 induced higher GATA3 expression, followed by enhanced GATA3 binding to the *ANXA1* promoter to inhibit *ANXA1* expression. In contrast, a moderate dosage of PGE2 increased CREB1 phosphorylation and reduced GATA3 binding to the *ANXA1* promoter, promoting *ANXA1* expression. We believe PGE2 and its regulatory target ANXA1 could be potential drugs for alkali-burned corneas.

INTRODUCTION

Chemical injury of the cornea is a true ocular emergency that requires immediate intervention.[1–3] Alkali burns, one of the leading causes of corneal blindness, can trigger a severe inflammatory response and cause extensive damage to the ocular surface and anterior segment. This can result in corneal complications such as epithelial defects, neovascularization, corneal fibrosis, necrosis, and perforation.[1–6] The treatment of corneal alkali burn remains a clinical challenge. Promoting rapid repair of the corneal epithelium and reducing the inflammatory response are key factors in corneal repair after an alkali burn.[1,2,5] Currently, anti-inflammatory drugs are the main drugs for treating corneal burns, supplemented by anti-infective, collagen, and ocular surface protective drugs.[2,6,7] Corticosteroids and non-steroidal anti-inflammatory drugs are commonly used in treating corneal inflammation. They can inhibit alkali-induced inflammation and neovascularization, but they are prone to corneal complications,[7–10] which is not conducive to wound healing.[4] Therefore, there is an urgent need to develop drugs that can reduce the inflammatory response and promote corneal epithelial repair.

ω-3 and ω-6 long-chain polyunsaturated fatty acids and their derivatives, such as arachidonic acid (AA), eicosapentaenoic acid (EPA), and docosahexaenoic acid (DHA), are abundant in corneas and involved in regulating the occurrence, development, and resolution of inflammation.[11–14] The injury induces the release of platelet-activating factor to stimulate AA to synthesize prostaglandins, triggering the inflammatory response.[4,15,16] A wide range of lipid mediators are released from immune and corneal cells to the injured site, actively coordinating the repair of the corneal epithelium.[16] The balance between pro-inflammatory and anti-inflammatory mediators ensures the orderly occurrence and regression of inflammation, and disrupting this balance leads to additional corneal damage.[12,17] Some studies suggest that the alkali burn causes lipid metabolism abnormalities in the cornea.[18]

Prostaglandin E2 (PGE2) is one of the major endogenous lipid mediators essential for maintaining tissue homeostasis under physiological conditions and plays a multifaceted role in the immune response under defined conditions.[14,19–22] PGE2 is produced by AA catalyzed by cyclooxygenase and PGE2 synthase.[21,23] PGE2 could activate endogenous stem cells,[19] regulate immunity,[20,23–25] promote angiogenesis,[26] and accelerate the regeneration and repair of multiple organs after injury.[21,27–29] Some investigations have indicated that PGE2 directs macrophages toward an anti-inflammatory phenotype, and inhibition of PGE2 production may lead to a shift in macrophage behavior and enhance

[1]Southwest Hospital/Southwest Eye Hospital, Third Military Medical University (Army Medical University), Chongqing 400038, China
[2]Key Lab of Visual Damage and Regeneration & Restoration of Chongqing, Chongqing 400038, China
[3]Army 953 Hospital, Shigatse Branch of Xinqiao Hospital, Third Military Medical University (Army Medical University), Shigatse 857000, China
[4]State Key Laboratory of Trauma, Burns, and Combined Injury, Department of Trauma Medical Center, Daping Hospital, Third Military Medical University (Army Medical University), Chongqing 400042, China
[5]Jinfeng Laboratory, Chongqing 401329, China
[6]These authors contributed equally
[7]Lead contact
*Correspondence: ccleqq@aliyun.com (B.B.), Liyijian2226@163.com (Y.L.), liuyy99@163.com (Y.L.)
https://doi.org/10.1016/j.isci.2023.108565

pro-inflammatory activity.[30–32] In addition, numerous studies have provided evidence that PGE2 can promote the regeneration and repair of skin, heart, intestines, and several therapeutic strategies based on PGE2 have been developed to facilitate the recovery of damaged tissues.[21,27–29,33] However, it remains unclear whether PGE2 is involved in corneal repair and inflammation resolution following an alkali burn.

To explore the potential use of PGE2 as a therapeutic agent for the treatment of alkali-burned corneas, different doses of PGE2 were administered to the alkali-burned corneas of mice and corneal epithelial cell lines. Distinct impacts of varying dose of PGE2 on corneal epithelial repair were observed. Furthermore, Annexin A1 (ANXA1) was identified as the primary target of PGE2 in promoting corneal epithelial repair after analyzing multiple transcriptomics data. Finally, the precise mechanism by which different doses of PGE2 regulate ANXA1 expression differently was elucidated. This study will lay a foundation for the development of PGE2 and its target as a drug for the treatment of alkali-burned corneas.

RESULTS

Alkali burn induces metabolic disorders, specifically in unsaturated fatty acids and immune imbalance

To explore the crucial targets involved in corneal repair after an alkali burn, we performed a transcriptome analysis using RNA-seq data[34] from corneas 7 days after alkali burn. Gene Set Enrichment Analysis (GESA) showed that the biological processes of "wound healing" and "leukocyte-mediated immunity" were significantly increased in the corneas after alkali burn. Interestingly, the biological functions of "metabolism of xenobiotics by cytochrome P450" and "arachidonic acid metabolism" in the corneas were reduced after an alkali burn (Figures 1A and S1A). Meanwhile, we found that the enrichment pathways of the downregulated differential expression genes (DEGs) in the corneas mainly included the "fatty acid metabolic process", "metabolism of xenobiotics by cytochrome P450" and "arachidonic acid metabolism" (Figures S1B and S1C). In contrast, the enrichment pathways of the upregulated DEGs were predominantly associated with the inflammatory response, specifically "leukocyte migration" and "cytokine-cytokine receptor interaction" (Figures S1B and S1D). The aforementioned findings suggest that there was a serious inflammatory response at 7 days after corneal alkali burns, accompanied by abnormal metabolism of fatty acids, specifically in arachidonic acid metabolism.

A moderate dosage of PGE2 promotes alkali-burned corneal epithelial repair, but a high dosage of PGE2 exerts a contrary effect

Given that PGE2 is a significant multifunctional metabolite of arachidonic acid,[14,20] we moved to explore the potential role of PGE2 in the repair of corneas after alkali burns. An alkali-burned model was established by treating the cornea with a 2 mm filter paper containing 0.2 M NaOH for 30 s. Subsequently, the mice were administered with 5 μL vehicle (0.1% DMSO) or PGE2 three times a day for four successive days (Figure 1B). The repair of the corneal epithelium was significantly improved with the application of 10 μM PGE2 treatment, as observed by fluorescein sodium staining, when compared to the control group. The former group was nearly healed on day 4 following an alkali burn, whereas the latter vehicle group showed a noticeable epithelial defect (Figures 1C and 1D). The results confirmed that PGE2 could promote corneal epithelial repair after an alkali burn, which is consistent with other reports indicating that PGE2 plays a role in promoting wound healing and regeneration.[21] However, surprisingly, the corneas treated with 250 μM PGE2 for four consecutive days did not effectively promote corneal epithelial repair. In contrast, it hindered corneal epithelial repair when compared to the 1% DMSO control group (Figures 1C and 1D). An upregulation of the inflammatory cytokines *Il1b*, *Il6*, and *Tnfa*, along with a downregulation of the immunomodulatory cytokine *Il10*, was observed in the alkali-burned corneas when compared to wild-type control corneas (Figure 1E). Notably, the expression of inflammatory cytokines was significantly reduced after 4 days of PGE2 treatment compared to the treatment with vehicle in the alkali-burned corneas, accompanied by an increased expression of *Il10* (Figure 1E). This effect is most pronounced in the group treated with 10 μM PGE2 (Figure 1E), which is consistent with the findings indicating that 10 μM PGE2 effectively promotes the wound healing of corneal epithelium.

To further understand the role of PGE2 in corneal repair, we initially examined the expression of PGE2 receptors and the metabolic enzymes involved in PGE2 synthesis using publicly available transcriptome data[34] from corneas with alkali burns compared to those without any burns. We found an increased expression of the PGE2 receptors *Ptger2* and *Ptger4*, as well as the enzymes *Ptges*, *Ptgs1*, and *Ptgs2*, which are involved in PGE2 synthesis (Figure 2A). This indicates that the PGE2-related pathway is activated following an alkali burn. Similarly, an upregulation of *Ptges*, *Ptgs1*, *Ptgs2*, and *Ptger2* expression was observed in the wounded corneas compared to normal corneas (Figure 2B). Together, these results suggest that PGE2 plays a vital role in the wound healing of the mice corneas.

Meanwhile, an *in vitro* scratch wound healing assay was conducted using human corneal epithelial cells (hCECs). We found that 10526, a specific inhibitor of PTGES, which suppresses the production of PGE2, significantly impeded the wound healing process of scratched hCECs when compared to the 0.1% DMSO controls (Figures 2C and 2D). This suggests that PGE2 plays a crucial role in the wound healing of hCECs. The percentages of wound healing in the treatment groups of 1 nM, 10 nM, and 100 nM were significantly higher compared to the 0.1% DMSO control group. In particular, the scratched areas of hCECs showed a notable reparative effect after treatment with 100 nM PGE2 (Figures 2E and 2F). However, the administration of higher dosages of PGE2, specifically 10 μM, 25 μM, and 50 μM, resulted in the inhibition of wound healing in scratched areas after 36 h (Figures 2E and 2F). The obtained results were in line with our *in vivo* findings, indicating that a moderate dosage of PGE2 can enhance corneal epithelial wound healing, while a higher dosage of PGE2 has an opposite effect. To distinguish these two opposite effects caused by different dosages of PGE2, we defined the dosage of PGE2 that can promote corneal epithelial repair as the moderate dosage, and the dosage of PGE2 that can inhibit corneal epithelial repair as the high dosage.

DmPGE2, a competitive inhibitor of HPGD that increases intracellular PGE2 levels,[27] was used to treat alkali-burned corneas both *in vivo* and in hCECs. A similar result was observed that 10 μM dmPGE2 promoted corneal epithelial wound healing *in vivo*, while 250 μM dmPGE2

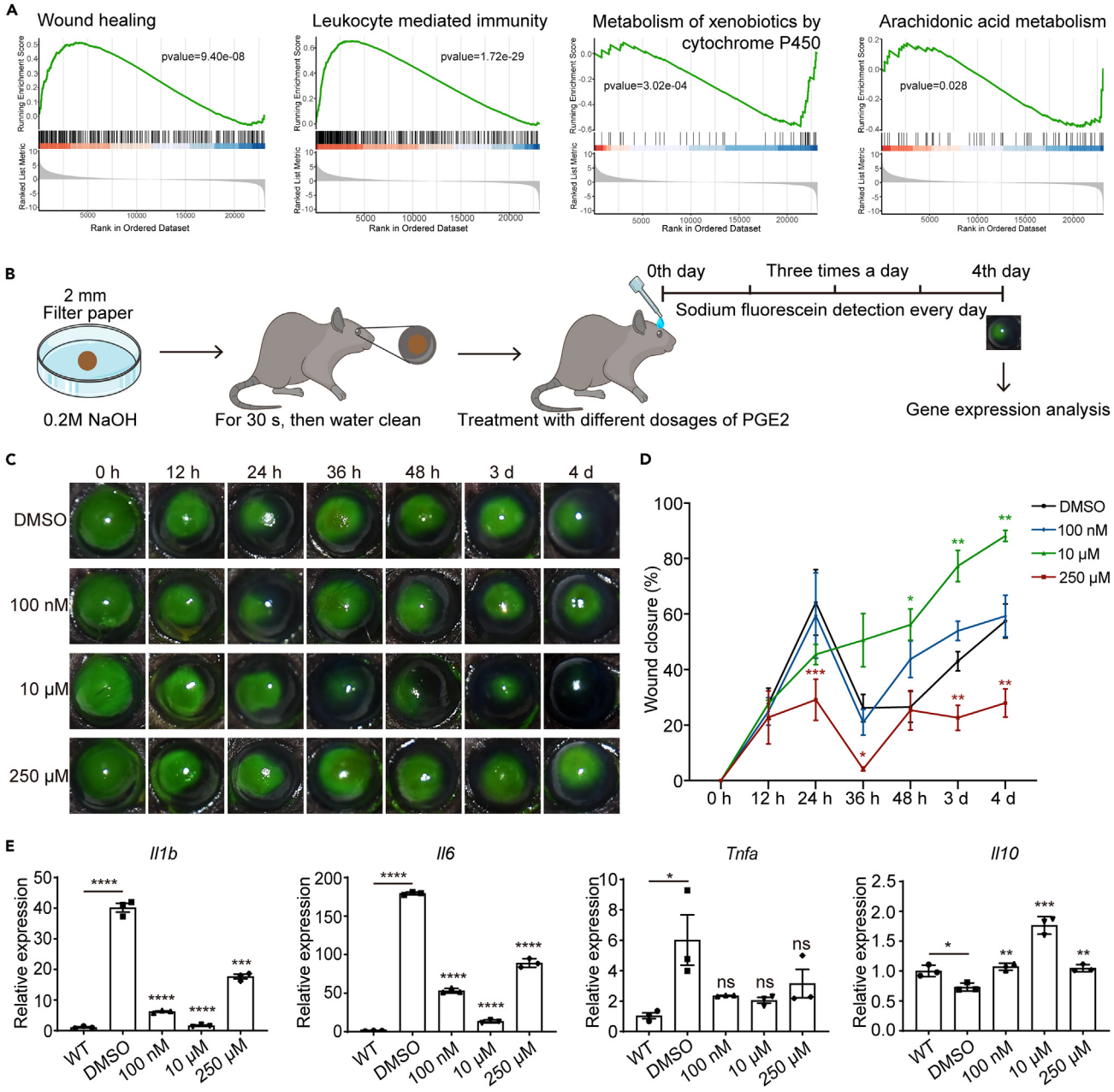

Figure 1. Effects of different dosages of PGE2 on the alkali-burned corneal epithelial repair

(A) Representative GSEA analysis terms for corneal genes between alkali-burned corneas vs. control corneas. The transcriptome data were downloaded from the SRA database.[34]

(B) Schematic overview of the alkali-burned cornea model and the administration of drugs.

(C and D) Representative images of fluorescein sodium staining (C) and statistical analysis (D) of corneal epithelial wound healing after alkali burns with different dosages of PGE2 treatment (n = 4).

(E) Gene expression analysis of *Il1b*, *Il6*, *Tnfa* and *Il10* on 4 days post alkali burns treated with different dosages of PGE2 (n = 3). Values are normalized to *Gapdh* and displayed relative to WT. 0.1% DMSO was used as the DMSO vehicle control. Error bars indicate mean ± SEM. *p < 0.05, **p < 0.01, ***p<0.001, ****p < 0.0001, and ns, no significance.

did not have the same effect (Figures S2A and S2B). In the *in vitro* experiment, the application of dmPGE2 at concentrations ranging from 1 nM to 25 μM, particularly at 10 μM, demonstrated a significant reparative effect on the wound healing process of hCECs. However, treatment with 50 μM dmPGE2 significantly inhibited the wound healing of scratched hCECs (Figures S2C and S2D). These results further confirm that a moderate dosage of PGE2 can effectively promote corneal epithelial wound healing, but a high dosage of PGE2 has the opposite effect.

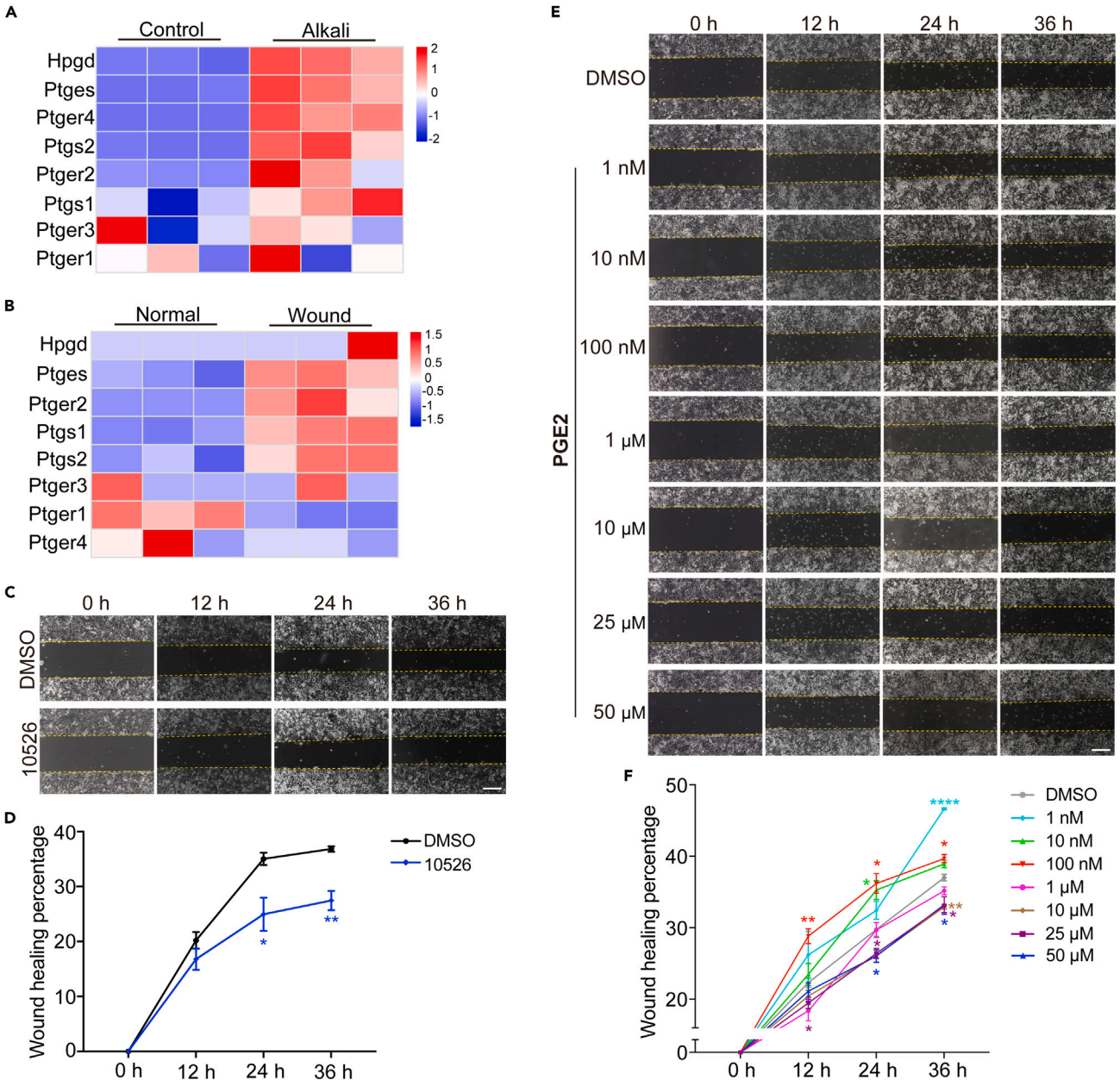

Figure 2. PGE2 is involved in the wound healing of corneal epithelium

(A) Heatmap shows the gene expression patterns of enzymes involved in the synthesis of PGE2, PGE2 receptors, and metabolic enzymes associated with PGE2 in alkali-burned corneas.

(B) Heatmap shows the gene expression patterns of enzymes involved in the synthesis of PGE2, PGE2 receptors, and metabolic enzymes associated with PGE2 in the wounded corneas.

(C and D) Representative images (C) and statistical analysis (D) of the wound healing of the scratch in hCECs after treatment with the inhibitor for PTGES (10526) (n = 3). Scale bar: 400 μm.

(E and F) Representative images (E) and statistical analysis (F) of the wound healing of the scratch in hCECs after treatment with different dosages of PGE2 (n = 3). 0.1% DMSO was used as the DMSO vehicle control. Error bars indicate mean ± SEM. *p < 0.05, **p < 0.01, and ****p < 0.0001.

PGE2 regulates the alkali-burned corneal epithelial wound healing via ANXA1

We have discovered that a moderate dosage of PGE2 promotes the repair of alkali-burned corneal epithelium. However, the exact mechanism of PGE2's function remains unclear. For this purpose, we conducted an analysis using previously published transcriptome data of intestinal organoids treated with 1 μM PGE2 vs. the control group (GEO database: GSE116936 [35]) and the corneas undergoing wound healing vs.

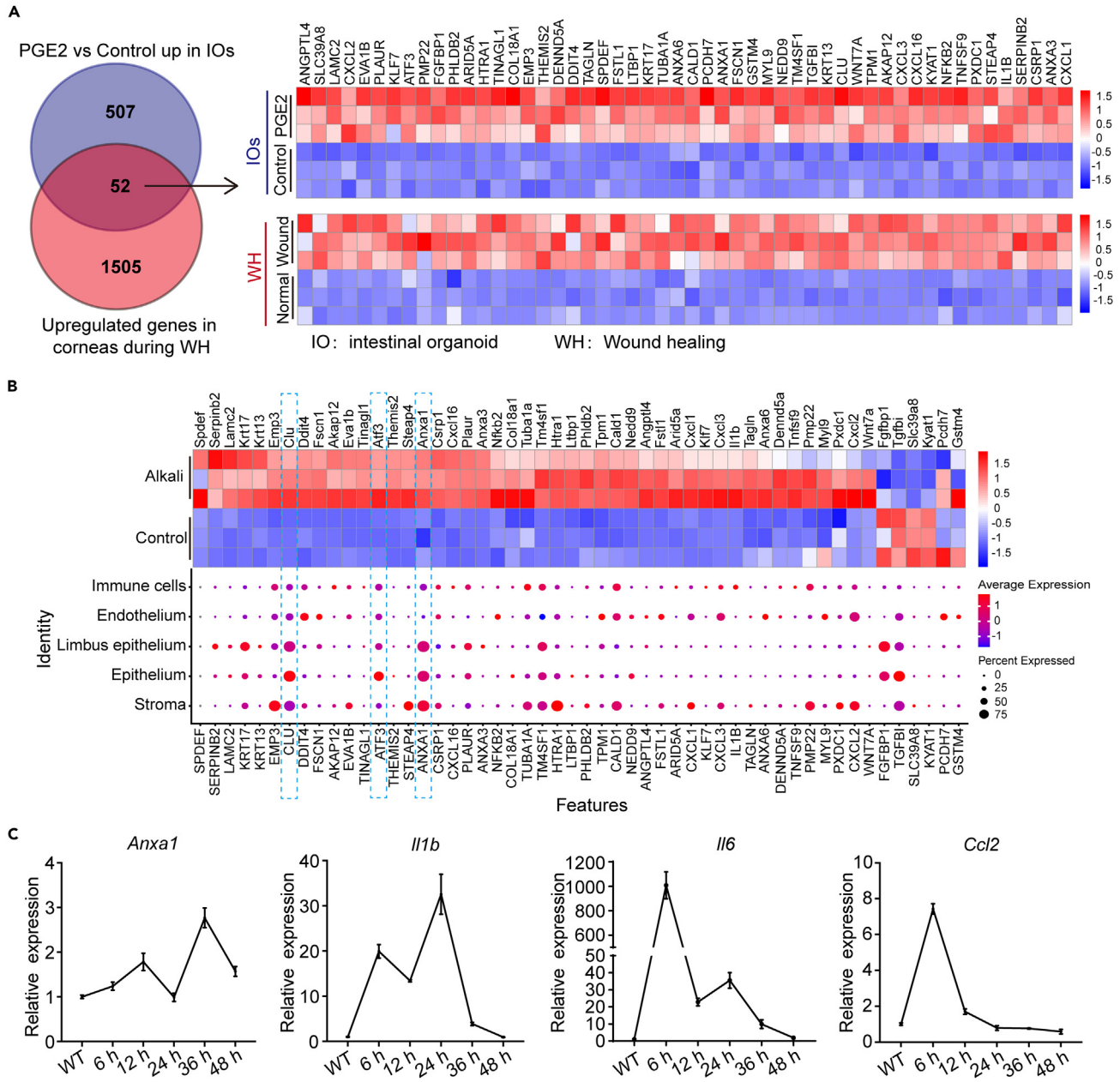

Figure 3. Identifying potential targets for PGE2 that promote corneal epithelial repair following alkali burns

(A) The Venn diagram of the significantly upregulated DEGs between the intestinal organoids (1 μM PGE2 vs. control) and the wounded corneas (wounded cornea vs. control). The transcriptome data was downloaded from the GEO database: GSE116936 [35] and the SRA database with the BioProject access number PRJNA669218[36]), respectively. Overlapped DGEs were plotted in a heatmap.

(B) The expression and distribution of the 52 overlapped DGEs in corneas. Upper: heatmap showing the 52 overlapped DGEs in alkali-burned corneas; Lower: dot plot showing the gene expression level and distribution in different corneal cells. The single-cell transcriptome data was downloaded from the GEO database: GSE186433.[37]

(C) Gene expression analysis of *Anxa1*, *Il1b*, *Il6*, and *Ccl2* in mice corneas at different time post alkali burns (n = 3). Values are normalized to GAPDH and displayed relative to WT. Error bars indicate mean ± SEM.

normal control corneas (BioProject database: PRJNA669218[36]). The analysis revealed a total of 52 overlapped upregulated DEGs (Figure 3A). Furthermore, it was observed that a majority of these 52 overlapped upregulated DEGs exhibited high expression levels in the alkali-induced corneas compared to the healthy corneas (Figure 3B). To analyze the expression of these 52 genes in different corneal cells, we performed a third data mining analysis using single-cell transcriptome data of corneas (GEO: GSE186433 [37]). Only *CLU*, *ATF3*, and *ANXA1* were highly

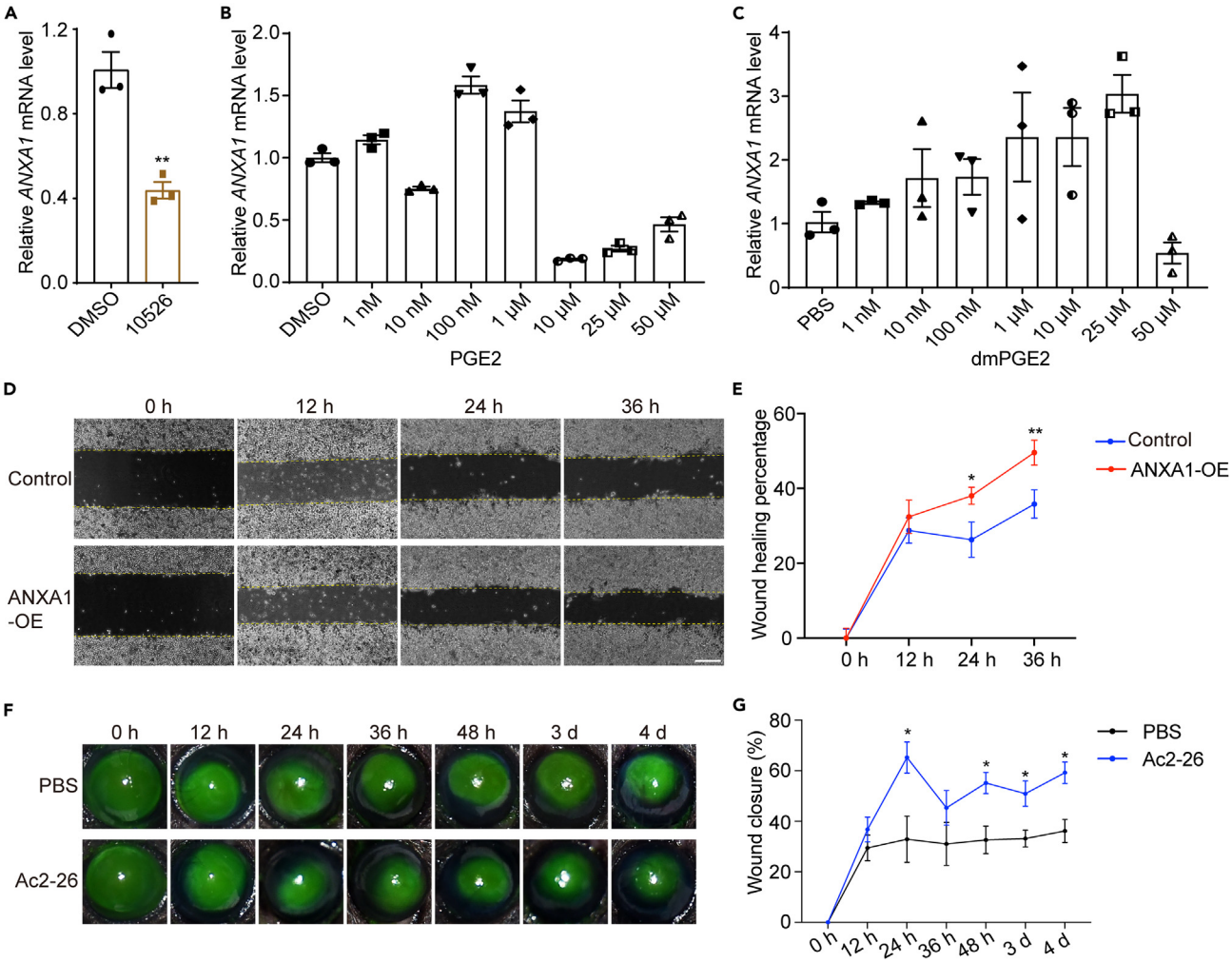

Figure 4. The effect of ANXA1 on the corneal epithelial repair after alkali burns and the ANXA1 expression response to different dosages of PGE2

(A) Gene expression analysis of *ANXA1* in hCECs after treatment with 10526 (n = 3). Values are normalized to GAPDH and displayed relative to the DMSO vehicle.

(B and C) Gene expression analysis of *ANXA1* in hCECs after treatment with different dosages of PGE2 (B) and dmPGE2 (C) (n = 3). Ordinary one-way ANOVA was used, $p < 0.0001$ in B and $p = 0.0052$ in C.

(D and E) Representative images (D) and statistical analysis (E) of the wound healing of the scratch in hCECs with the overexpression of *ANXA1* (n = 3). Scale bar: 400 μm.

(F and G) Representative images of fluorescein sodium staining (F) and statistical analysis (G) of corneal epithelial wound healing after alkali burn with the treatment of a mimetic peptide of ANXA1 (Ac2-26) (n = 4). 0.1% DMSO was used as the DMSO vehicle control, and PBS was used as the PBS vehicle control. Error bars indicate mean ± SEM. *$p < 0.05$, and **$p < 0.01$.

expressed in the majority of corneal epithelial cells, especially *CLU* and *ANXA1* (Figure 3B). *CLU* is involved in cell death, tumor progression, and neurodegenerative disorders.[38] *ANXA1*, a crucial anti-inflammatory protein,[39] is reported to promote tumor progression[40] and the repair of corneal scarring.[41,42] Since *ANXA1* is more closely associated with the cornea, we, therefore, are focused on *ANXA1*. And we found *Anxa1* was highly expressed at 36 h after alkali burns, accompanied by a significant downregulation of inflammatory cytokines *Il1b* and *Il6*, as well as chemokines *Ccl2* (Figure 3C). So, we hypothesize that ANXA1 functions as a potential target for a moderate dosage of PGE2 to promote corneal epithelial repair and accelerate the regression of corneal inflammation.

The expression of *ANXA1* at the transcriptional level in hCECs was observed to be downregulated by approximately 60% following treatment with 10526 (Figure 4A). We found *ANXA1* expression was promoted by PGE2 at concentrations of 100 nM and 1 μM. However, higher concentrations of PGE2 (10 μM, 25 μM, and 50 μM) inhibited *ANXA1*expression (Figure 4B). Consistent with previous findings, the administration of a high dosage of dmPGE2 (50 μM) resulted in the inhibition of *ANXA1* expression (Figure 4C). These results indicate that a moderate dosage of PGE2 can enhance *ANXA1* expression, whereas a high dosage of PGE2 has a suppressive effect on *ANXA1* expression. To further explore the role of ANXA1 in alkali-burned corneal epithelium, *ANXA1* was overexpressed in hCECs (Figure S3) and we found *ANXA1* overexpression significantly promoted the wound healing of scratched hCECs at 24 h and 36 h, as compared to controls (Figures 4D and 4E).

Ac2-26, a synthesized peptide of the N-terminus of ANXA1 protein with 25 amino acids from 2 to 26, has demonstrated comparable biological activities to those of the full-length ANXA1 protein,[41,43] significantly promoted the corneal epithelial wound healing at 24 h after treatment which persisted to 4 days after alkali burns (Figures 4F and 4G). Based on these results, we confirm that a moderate dosage of PGE2 promotes *ANXA1* expression, thus promoting the wound healing of the corneal epithelium; in contrast, a high dosage of PGE2 has the opposite effect.

A high dosage of PGE2 inhibits *ANXA1* promoter via a *cis*-regulatory element of GATA3 located at −900 bp—-1000 bp of the *ANXA1* promoter

Promoters play a critical role in the regulation of gene expression. To explore whether PGE2 regulates *ANXA1* expression through the *ANXA1* promoter, we evaluated the 2000 bp (−2000 to +100) upstream sequence from the transcription initiation site of both human *ANXA1* and mouse *Anxa1* to predict the binding sites for transcription factors by the JASPAR database.[44] We found many *cis*-acting regulatory elements (CREs) for PGE2-related transcription factors in the *ANXA1* promoter (Tables S1 and S2), including Fos and NFAT1, which might be regulated by PGE2 and its receptor.[45,46] It was indicated that PGE2 could upregulate *ANXA1* expression through these transcription factors. We constructed a dual luciferase reporter vector containing the 2000 bp promoter sequence of the human *ANXA1* gene and transfected it into hCECs. The subsequent experiments used a human *ANXA1* promoter, unless otherwise specified. Dual luciferase results showed that 1 nM and 1 μM PGE2 significantly enhanced the activity of the *ANXA1* promoter; by contrast, 50 μM PGE2 inhibited the activity of the *ANXA1* promoter (Figure 5A). These results indicate that different dosages of PGE2 can directly act upon the *ANXA1* promoter to enhance or inhibit *ANXA1* expression.

To identify the specific CREs affected by a high dosage of PGE2 in inhibiting *ANXA1* expression, we sequentially subtracted some loci of the 2000 bp *ANXA1* upstream sequence and constructed four luciferase reporter vectors that were 500 bp, 1000 bp, 1500 bp, and 2000 bp in length. We observed that 1 nM PGE2 enhanced the activity of the *ANXA1* promoter at all four vectors. In contrast, the *ANXA1* promoter activity was not enhanced by a high dosage of PGE2 with a concentration of 50 μM when using the 1000 bp and 2000 bp vectors. It even inhibited the activity of the *ANXA1* promoter at the 1000 bp and 2000 bp vectors (Figure 5B). These results suggest that a high dosage of PGE2 inhibits the activity of *ANXA1* promoter primarily through *cis*-regulatory elements located within the -500—-1000 bp upstream region of the *ANXA1* promoter. Subsequently, we further truncated the 1000 bp upstream sequence of *ANXA1* and constructed the luciferase reporter vector. The results show that a high dosage of PGE2 significantly inhibits the activity of the *ANXA1* promoter within the 800 bp and 1000 bp upstream regions. However, the inhibition by a high dosage of PGE2 on the activity of the *ANXA1* promoter with 900 bp regions was not significantly (Figure 5C). Based on these results, it is postulated that the critical *cis*-regulatory elements affected by a high dosage of PGE2 are most likely located within the -700—-800 bp and -900—-1000 bp regions of the *ANXA1* promoter.

Then we performed an in-depth analysis of the sequences located in -700—-800 bp and -900—-1000 bp of the *ANXA1* promoter. A total of 23 transcription factors were predicted as potential factors that can bind to the analyzed sequences. Notably, the predicted binding elements of GATA3 and FOXL1 were found to be present in both -700—-800 bp and -900—-1000 bp of the *ANXA1* promoter (Figure 5D, Table S3). While four FOXL1 CREs were predicted within the 500 bp upstream sequence of the *ANXA1* promoter (Table S4), a high dosage of PGE2 did not significantly inhibit the activity of the 500 bp *ANXA1* promoter. Therefore, we believed that the elements which are responded to a high dosage of PGE2 and inhibit promoter activity are not the binding element of FOXL1. The binding element of GATA3 is most likely to contribute to a high dosage of PGE2 that inhibits the *ANXA1* promoter. GATA3 belongs to the zinc-binding transcription factor, which regulates differentiation,[47] immunity,[48] and promotes tumor invasion.[49] To investigate the effect of GATA3 on ANXA1 expression, we constructed a GATA3 overexpression vector and transfected it into hCECs. We found the overexpression of GATA3 could downregulate the expression of ANXA1 (Figure 5E). Similarly, the analysis of RNA-seq data (GEO database: GSE216413) revealed that the overexpression of GATA3 significantly reduced the expression of *ANXA1* in breast cancer cells (Figures S4A and S4B). Transcriptome data (GEO database: GSE190381 [50]) of the luminal breast cancer cell lines with *GATA3* mutation revealed a notable upregulation in *ANXA1* expression (Figure S4C). These data suggest that GATA3 can inhibit ANXA1 expression.

Two GATA3 CRE were predicted at -700—-800 bp and -900—-1000, including the putative GATA3 CRE1 located at -782—-777 and GATA3 CRE2 located at -914—-909 of the *ANXA1* promoter (Figure 5D). We performed mutagenesis on GATA3 CRE1 and CRE2 to construct the corresponding luciferase reporter vectors. These vectors were then co-transfected with a GATA3 overexpression vector into hCECs. Luciferase activity analysis showed that both the unmutated vector and the GATA3 CRE1 mutated vector exhibited the ability to inhibit the activity of the *ANXA1* promoter. However, the GATA3 CRE2 mutated vector did not exhibit this inhibitory effect (Figure 5F). These results together indicate that GATA3 inhibits the activity of the *ANXA1* promoter through the GATA3 CRE2.

A high dosage of PGE2 inhibits ANXA1 by enhancing GATA3 expression and the moderate dosage of PGE2 promotes ANXA1 by increasing CREB1 phosphorylation

Luciferase activity analysis indicated that the mutation of GATA3 CRE1 or GATA3 CRE2 did not eliminate the inhibitory effect of a high dosage of PGE2 on the *ANXA1* promoter (Figure 6A). This suggests the presence of additional elements that respond to a high dosage of PGE2 and contribute to the inhibition of *ANXA1* promoter activity. PGE2 triggers different signaling pathways through four G protein-coupled receptors (EP1-EP4), thus mediating various biological functions.[51,52] EP2 and EP4 can activate adenylate cyclase (AC) through the activation of Gs protein, resulting in an increase in cyclic adenosine monophosphate (cAMP) levels. While cAMP can allosterically activate protein kinase A (PKA) to enhance the phosphorylation of cAMP response element binding protein (CREB), thereby inducing the expression of target genes downstream.[53] The EP3 receptor subtype couples to the Gi protein to inhibit the cAMP pathway and subsequently reduces CREB

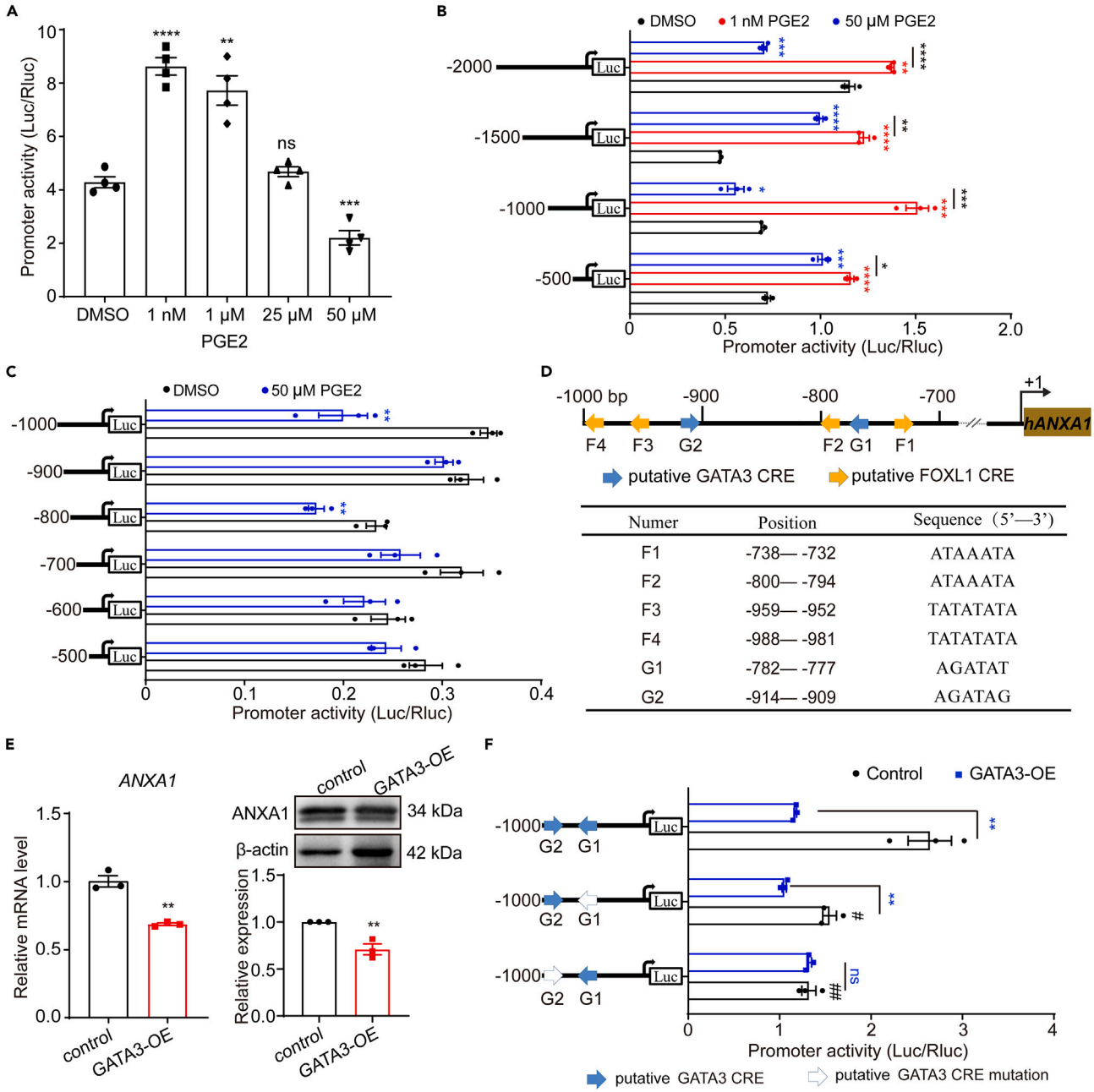

Numer	Position	Sequence (5'—3')
F1	-738— -732	ATAAATA
F2	-800— -794	ATAAATA
F3	-959— -952	TATATATA
F4	-988— -981	TATATATA
G1	-782— -777	AGATAT
G2	-914— -909	AGATAG

Figure 5. Screening the target elements contributing to a high dosage of PGE2 inhibiting the activity of the *ANXA1* promoter

(A) The analysis of different dosages of PGE2 on the activity of the *ANXA1* promoter. The 2000 bp *ANXA1* promoter was used as the full-length promoter for analysis by dual luciferase activity assay (n = 4).

(B) Effects of a moderate dosage and a high dosage of PGE2 on the activity of the *ANXA1* promoters with different lengths. The 2000 bp *ANXA1* promoter was shortened to four lengths with an interval of 500 bp (n = 3).

(C) Effects of a high dosage of PGE2 on the activity of the *ANXA1* promoter with different lengths. The 1000 bp *ANXA1* promoter was shortened to 500 bp, 600 bp, 700 bp, 800 bp, 900 bp, and 1000 bp with an interval of 100 bp (n = 3).

(D) Schematic illustration of the predicted cis regulate elements (CREs) located in -700—-800 bp and -900—-1000 bp of the *ANXA1* promoter. "+1" represents the transcription start site.

(E) The ANXA1 expression analysis after the overexpression of GATA3 in hCECs (n = 3). qPCR and western blot were used. Values are normalized to GAPDH and β-actin and displayed relative to the empty vector control, respectively.

(F) Effects of GATA3 on the luciferase activity of the 1000 bp *ANXA1* promoter with the predicted GATA3 CRE1 and CRE2 mutation (n = 3). The activity of *ANXA1* promoter with the mutation of GATA3 CRE1 and CRE2 was compared with the control *ANXA1* promoter. #p < 0.05, ##p < 0.01. The activity of *ANXA1* promoter with the overexpression of GATA3 was compared with the corresponding control group. 0.1% DMSO was used as the DMSO vehicle control. Error bars indicate mean±SEM. *p < 0.05, **p < 0.01, ***p<0.001, ****p < 0.0001, and ns, no significance.

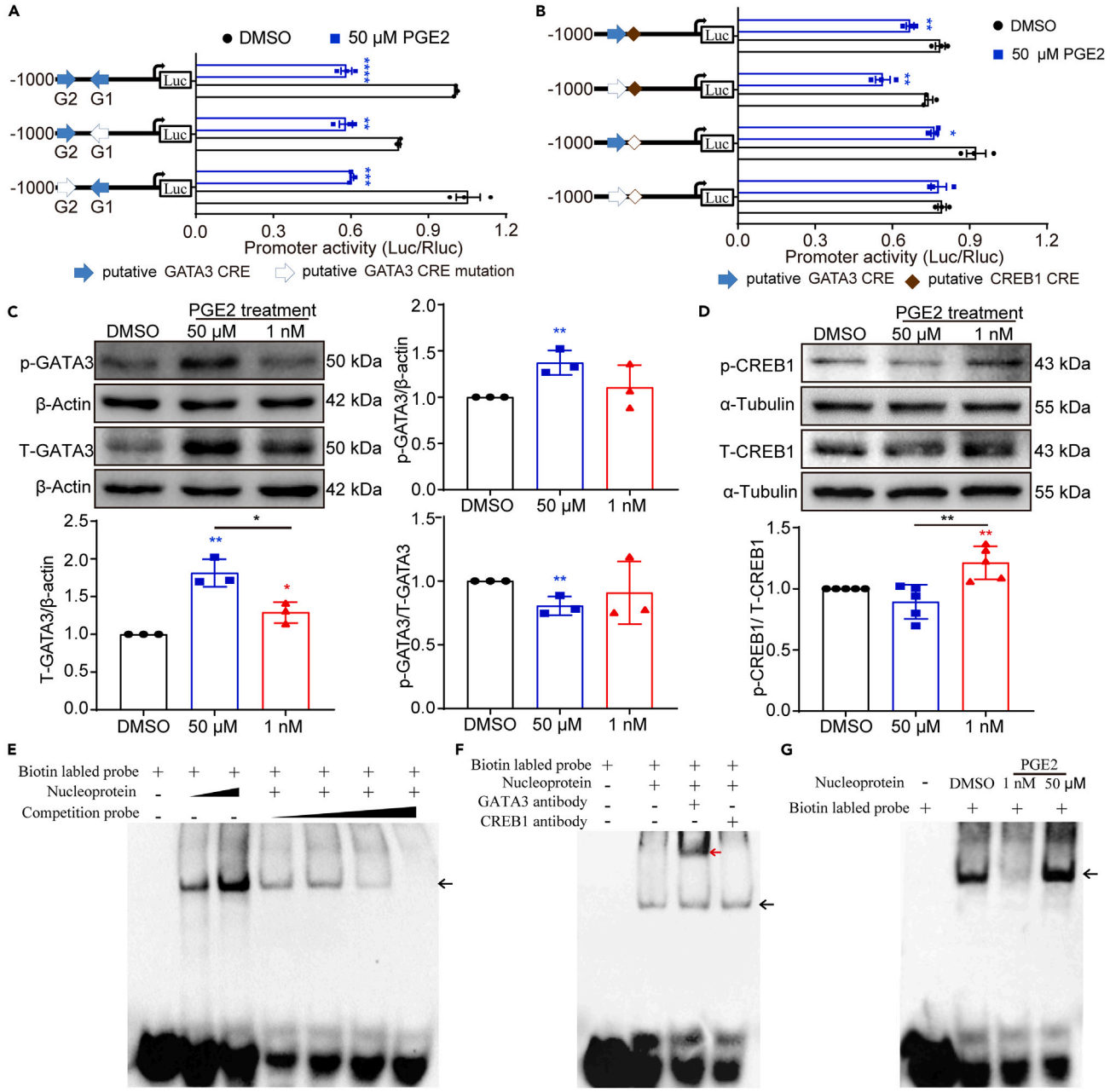

Figure 6. A high dosage of PGE2 inhibited ANXA1 expression by enhancing GATA3 expression and reducing CREB1 phosphorylation

(A) Effects of a high dosage of PGE2 on the activity of the 1000 bp *ANXA1* promoter with the mutation of predicted GATA3 CRE1 and CRE2 (n = 3).

(B) Effects of a high dosage of PGE2 on the activity of the 1000 bp *ANXA1* promoter with the mutation of predicted GATA3 CRE2 and CREB1 CRE. The arrows and diamonds filled with white indicate the corresponding CRE mutations.

(C) Analysis of GATA3 expression and phosphorylation in hCECs after treatment with different dosages of PGE2.

(D) Analysis of CREB1 phosphorylation in hCECs after treatment with different dosages of PGE2.

(E) The binding analysis of the nucleoproteins of hCECs with the GATA3 CRE2 and CREB1 CRE probe by electrophoretic mobility shift assays. GATA3 CRE2 and CREB1 CRE probe concentrations were 1 μM; nucleoprotein proteins were 2.5μg and 12.5 μg, respectively; the concentrations of competing probes were 100 nM, 250 nM, 2.5 μM, and 25 μM.

(F) The binding analysis of the nucleoproteins of hCECs with the probes after co-incubation with GATA3 antibody. The probe concentration was 1 μM; Nucleoprotein protein was 10 μg; antibody was 1 μg, respectively.

(G) The binding analysis of the nucleoproteins of hCECs after treatment with different dosages of PGE2 with probes by electrophoretic mobility shift assays. The probe concentration was 1 μM; the nucleoprotein protein was 10 μg. 0.1% DMSO was used as the DMSO vehicle control. Error bars indicate mean±SEM. *p < 0.05, **p < 0.01, ***p<0.001, and ****p < 0.0001.

phosphorylation.[52] Some studies have indicated that a low dosage of PGE2 promoted the phosphorylation of CREB, whereas a high dosage of PGE2 inhibited it.[54] Our previous predictions suggested that a potential CREB1 binding site adjacent to GATA3 CRE2. Would this site contribute to the inhibition of *ANXA1* promoter activity in response to a high dosage of PGE2? We mutated the CREB1 CRE and found that mutations in either GATA3 CRE2 or CREB1 CRE alone did not fully eliminate the inhibitory effect of a high dosage of PGE2 on the activity of the *ANXA1* promoter (Figure 6B). However, a high dosage of PGE2 no longer inhibited the activity of the *ANXA1* promoter with double mutations of GATA3 CRE2 and CREB1 CRE (Figure 6B). Therefore, we were convinced that a high dosage of PGE2 inhibited the activity of the *ANXA1* promoter through the synergistic effect of GATA3 CRE2 and CREB1 CRE. Western blotting analysis revealed a higher GATA3 expression following treatment with a high dosage PGE2; While, a moderate dosage of PGE2 resulted in increased phosphorylation of CREB1 (Figures 6C and 6D). Taken collectively, when compared to a moderate dosage of PGE2, a high dosage of PGE2 was found to inhibit the expression of ANXA1 by enhancing the expression of GATA3 and reducing the phosphorylation of CREB1.

To examine the potential binding of GATA3 and CREB1 to GATA3 CRE2 and CREB1 CRE on the *ANXA1* promoter, we synthesized a biotin-labeled probe containing both GATA3 CRE2 and CREB1 CRE to perform electrophoretic mobility shift assays (EMSAs). The results showed apparent lag bands was formed upon incubation of the biotin-labeled probes with the nucleoproteins of hCECs (Figure 6E). The lag bands were gradually enhanced when the nucleoproteins of hCECs were increased; in contrast, the signal was gradually weakened with the addition of competitive probes (Figure 6E), indicating that certain nucleoproteins could specially bind to the probe containing GATA3 CRE2 and CREB1 CRE. Then the antibody specific to GATA3 and CREB1 was employed to co-incubate with the probe and nucleoprotein. A super-lag band was observed upon the addition of GATA3 antibody, but no super-lag band was observed when the CREB1 antibody was added (Figure 6F). These results indicate that GATA3, rather than CREB1, is the protein in the nucleoprotein complex that binds to the biotin-labeled probe. In addition, we also found the lag band of GATA3 binding to the probe was enhanced when the CREB1 antibody was added (Figure 6F), suggesting that CREB1 may exert an inhibitory effect on the binding of GATA3 to the *ANXA1* promoter. Finally, we explored the binding of nucleoprotein treated with a moderate and a high dosage of PGE2 to the GATA3 CRE2 and CREB1 CRE probes. The binding lag band of the nucleoprotein treated with a high dosage of PGE2 was obviously enhanced compared with that in 0.1% DMSO control group (Figure 6G). However, the binding lag band of the nucleoprotein treated with a moderate dosage of PGE2 to the probe was significantly weakened compared with that in 0.1% DMSO control group (Figure 6G). These findings demonstrate that a high dosage of PGE2 stimulates GATA3 expression, thereby enhances the binding of GATA3 to the *ANXA1* promoter and subsequently inhibiting ANXA1 expression. In contrast, a moderate dosage of PGE2 increases the phosphorylation of CREB1, interfering with the binding of GATA3 to the *ANXA1* promoter, ultimately leading to the upregulation of ANXA1expression.

DISCUSSION

A moderate dosage of PGE2 serves as a potential therapeutic drug for alkali-burned cornea

This study discovered that corneal alkali burn induces abnormal AA metabolism and triggers a severe inflammatory response. A recent study has demonstrated that Lipoxin A4 (LXA4), a downstream lipid mediator of AA, can reduce corneal inflammation and neovascularization.[4] Additionally, previous reports that PGE2, which is also a crucial downstream lipid mediator of AA,[14,22] can promote the tissues and organs regeneration.[21,27–29,55] We found a moderate dosage of PGE2 could promote the repair of corneal epithelium and reduce corneal inflammation after alkali burns. So, the administration of the moderate dosage of PGE2 could potentially serve as a therapeutic drug for the treatment of alkali-burned corneas. Interestingly, our findings revealed that a high dosage of PGE2 exhibited an opposite effect, which inhibited corneal epithelial repair. Several studies have shown that PGE2 can promote the formation of neovascularization.[56] Whether there is a dose-dependent effect of PGE2 on promoting corneal neovascularization (CNV) formation and whether there is a balance between facilitating the corneal epithelial repair and the development of CNV following an alkali burn remains unclear. We did not observe the formation of CNV in the alkali burn model induced by 0.2 M NaOH during the application of PGE2. Notably, the pathophysiology of severe corneal alkali burn is more complex when compared to the alkali burn model induced by 0.2 M NaOH. These severe burns are often accompanied by the development of CNV. The selection of therapeutic drugs is influenced by the severity of corneal alkali burns. Therefore, a comprehensive investigation is needed to examine the effects of PGE2 on corneal repair in cases of severe alkali burns in the future. Additionally, PGE2 can enhance stem cell function,[19] so it's reasonable to integrate the effects of PGE2 on maintaining stem cells and regulating inflammation to facilitate the repair of alkali-burned corneas by stem cell transplantation.

A high dosage of PGE2 causes a side effect on corneal epithelial repair follow an alkali burn through inhibiting ANXA1 expression

Prostaglandins are widely used drugs in the treatment of glaucoma[57] and latanoprost exerts its therapeutic effects through acting on PGF2α.[58] However, the long-term or excessive utilization of prostaglandins may cause certain side effects,[58] consistent with our findings that a high dosage of PGE2 hinders corneal repair after an alkali burn. We, therefore, are interested in the underlying reasons for the divergent findings observed in corneal epithelial repair when different dosages of PGE2 are administered. Although different tissues or organs may exhibit different responses to a same drug, we expect to find a shared mechanism for the repair effect induced by PGE2. We screened out ANXA1 as a target of PGE2 that promotes corneal repair by multiple data analysis. Several studies[59] have demonstrated that Phospholipase A2 can interact with ANXA1 to promoting tumorigenesis and cancer aggressiveness. The results of our study suggested the expression of ANXA1 can be regulated by PGE2. Specifically, our observations indicate that a moderate dosage of PGE2 induces an upregulation of ANXA1 expression, whereas a high dosage of PGE2 inhibits ANXA1 expression. Studies have shown that LXA4 can reduce obesity-induced

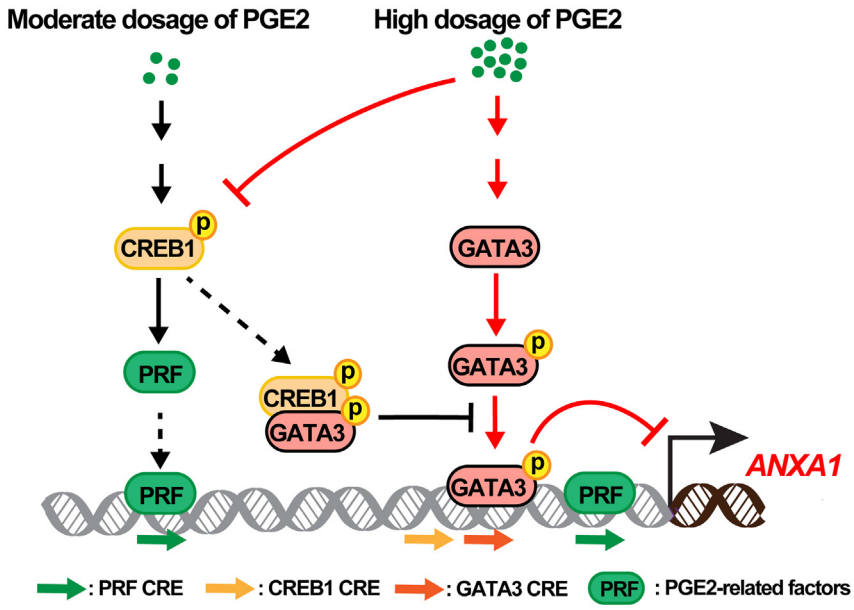

Figure 7. Schematic diagrams to elucidate the molecular mechanism of different dosages of PGE2 regulate the differential expression of ANXA1

adipose inflammation by increasing ANXA1 expression.[60] Additionally, there is a crosstalk between PGE2 and LXA4.[61] This crosstalk and antagonistic regulation between ANXA1 and PGE2 may contribute to the timely and orderly regression of inflammation.

A moderate dosage of PGE2 may promote CREB1 phosphorylation to increase ANXA1 expression by binding with EP2

Recent studies have indicated that PGE2 signals negatively influence MEF2A transcriptionally regulated IFN I synthesis and have raised the possibility that PGE2-cAMP-eliciting environmental cues in macrophages downregulate MEF2A-dependent inflammatory gene expression.[24] We predicted a possible MEF2A CRE on *ANXA1* promoter. But a high dosage of PGE2 could not inhibit the activity of the *ANXA1* promoter through the predicted CRE (data not shown). In our study, we predicted a CREB1 CRE located next to the GATA3 CRE2, which could synergistically respond to a high dosage of PGE2 along with GATA3 CRE2 to inhibit the activity of the *ANXA1* promoter. PGE2 has been widely recognized for its ability to stimulate the phosphorylation of CREB through its binding to EP2 and EP4 receptors.[53] And we found only EP2 was upregulated in the corneas 7 days after alkali burn and 16 h after an injury during wound healing, suggesting that PGE2 may play an important role by binding to EP2 to promote the phosphorylation of CREB during the wound healing in the cornea.

CREB1 and GATA3 synergistically respond to different dosages of PGE2 to regulate *ANXA1* expression

In this study, we observed the dose-dependent effect of PGE2 on corneal epithelial repair was mediated by the differential transcriptional regulation of *ANXA1*. A moderate dosage of PGE2 can increase ANXA1 expression to promote corneal epithelial repair, but a high dosage of PGE2 inhibits corneal epithelial repair by inhibiting ANXA1 expression. And we were fortunate to discover that the effect was controlled by the neighboring GATA3 CRE2 and CREB1 CRE. Specifically, a high dosage of PGE2 induces higher GATA3 expression to enhance GATA3 bind to *ANXA1* promoter, inhibiting ANXA1 expression. Oppositely, a moderate dosage of PGE2 enhances the phosphorylation of CREB1, potentially interfering with the binding of GATA3 to the *ANXA1* promoter, ultimately resulting in the upregulation of ANXA1 expression (Figure 7). These findings elucidate the molecular regulatory mechanism of ANXA1 expression mediated by PGE2 during the process of corneal epithelial repair, laying a foundation for exploring an effective therapeutic target for treating alkali-burned corneas.

Limitations of the study

We did not verify the therapeutic effect of PGE2 under different degrees of alkali-induced corneal injury. And this study only demonstrated a moderate dosage of PGE2 has the potential to serve as a therapeutic drug for the treatment of corneal alkali damage, but further investigation is required to determine the specific optimal dosage to apply for the treatment of corneal alkali damage. ANXA1 represents one of the primary targets of PGE2 in promoting the repair of the alkali-burned corneas at a moderate dosage of PGE2, we did not provide further clarification on the existence of other potential targets. We focused on the mechanism by which a high dosage of PGE2 inhibits *ANXA1* expression, while not addressing the precise molecular mechanism by which a moderate dosage of PGE2 promotes *ANXA1* expression. In addition, our study only confirmed that CREB1 could affect the binding of GATA3 to the ANXA1 promotors, but did not clarify the specific mechanism and the interaction between GATA3 and CREB1, which will be the primary focus of our future investigations.

STAR★METHODS

Detailed methods are provided in the online version of this paper and include the following:

- KEY RESOURCES TABLE
- RESOURCE AVAILABILITY
  - Lead contact
  - Materials availability
  - Data and code availability
- EXPERIMENTAL MODEL AND STUDY PARTICIPANT DETAILS
  - Cell lines
  - *In vivo* mouse studies
  - Plasmids
  - Bacterial strains
  - Chemical reagents
- METHOD DETAILS
  - Alkali-induced corneal injury
  - Fluorescein sodium staining
  - Drug's treatment
  - RNA extraction and quantitative real time PCR (qPCR)
  - Single-cell RNA-seq and bulk RNA-seq analysis
  - *In vitro* scratch wound healing assay
  - Vector constructions
  - Western blot
  - Dual luciferase reporter assay
  - Electrophoretic mobility-shift assay (EMSA)
- QUANTIFICATION AND STATISTICAL ANALYSIS

SUPPLEMENTAL INFORMATION

Supplemental information can be found online at https://doi.org/10.1016/j.isci.2023.108565.

ACKNOWLEDGMENTS

This work was supported by the National Natural Science Foundation of China (81970843 to Y.L., 82271132 to Y.L., and 82101167 to B.B.); the Chongqing Postdoctoral Science Special Foundation (4142ZA078 to H.L.), and the Natural Science Foundation project of Chongqing (CSTB2022NSCQ-MSX1041 to B.B.).

AUTHOR CONTRIBUTIONS

H.L. and X.Z.: Conceptualization, Methodology, Software, Data curation, Writing – original draft, Writing - review and editing. Q.T.: Resources, Software, Formal analysis. L.G., J.L., and C.R.: Investigation, Validation, Software. Y.L.: Writing – review and editing, Supervision. B.B. and Y.L.: Funding acquisition, Supervision.

DECLARATION OF INTERESTS

The authors declare no competing interests.

Received: September 7, 2023
Revised: October 14, 2023
Accepted: November 21, 2023
Published: November 23, 2023

REFERENCES

1. Wagoner, M.D. (1997). Chemical injuries of the eye: current concepts in pathophysiology and therapy. Surv. Ophthalmol. *41*, 275–313.
2. Sharma, N., Kaur, M., Agarwal, T., Sangwan, V.S., and Vajpayee, R.B. (2018). Treatment of acute ocular chemical burns. Surv. Ophthalmol. *63*, 214–235.
3. Bizrah, M., Yusuf, A., and Ahmad, S. (2019). An update on chemical eye burns. Eye (Lond) *33*, 1362–1377.
4. He, J., Pham, T.L., Kakazu, A.H., Ponnath, A., Do, K.V., and Bazan, H.E.P. (2023). Lipoxin A4 (LXA4) Reduces Alkali-Induced Corneal Inflammation and Neovascularization and Upregulates a Repair Transcriptome. Biomolecules *13*, 831.
5. Baradaran-Rafii, A., Eslani, M., Haq, Z., Shirzadeh, E., Huvard, M.J., and Djalilian, A.R. (2017). Current and Upcoming Therapies for Ocular Surface Chemical Injuries. Ocul. Surf. *15*, 48–64.

6. Liang, W., Zhang, Y., Zhou, L., Lu, X., Finn, M.E., Wang, W., Shao, H., Dean, D.C., Zhang, L., and Liu, Y. (2022). Zeb1 regulation of wound-healing-induced inflammation in alkali-damaged corneas. iScience *25*, 104038.
7. Cornea Group of Ophthalmology Branch of Chinese Medical Association (2021). [Expert consensus on the clinical diagnosis and treatment of eye burns in China (2021)]. Zhonghua. Yan Ke Za Zhi. *57*, 254–260.
8. Gueudry, J., Lebel, H., and Muraine, M. (2010). Severe corneal complications associated with topical indomethacin use. Br. J. Ophthalmol. *94*, 133–134.
9. Jones, L., Downie, L.E., Korb, D., Benitez-Del-Castillo, J.M., Dana, R., Deng, S.X., Dong, P.N., Geerling, G., Hida, R.Y., Liu, Y., et al. (2017). TFOS DEWS II Management and Therapy Report. Ocul. Surf. *15*, 575–628.
10. Donshik, P.C., Berman, M.B., Dohlman, C.H., Gage, J., and Rose, J. (1978). Effect of topical corticosteroids on ulceration in alkali-burned corneas. Arch. Ophthalmol. *96*, 2117–2120.
11. Gronert, K. (2005). Lipoxins in the eye and their role in wound healing. Prostaglandins Leukot. Essent. Fatty Acids *73*, 221–229.
12. Brennan, E., Kantharidis, P., Cooper, M.E., and Godson, C. (2021). Pro-resolving lipid mediators: regulators of inflammation, metabolism and kidney function. Nat. Rev. Nephrol. *17*, 725–739.
13. Wang, W., Zhu, J., Lyu, F., Panigrahy, D., Ferrara, K.W., Hammock, B., and Zhang, G. (2014). ω-3 polyunsaturated fatty acids-derived lipid metabolites on angiogenesis, inflammation and cancer. Prostag. Other Lipid Mediat. *113–115*, 13–20.
14. Theken, K.N., and FitzGerald, G.A. (2021). Bioactive lipids in antiviral immunity. Science *371*, 237–238.
15. Bazan, H., and Ottino, P. (2002). The role of platelet-activating factor in the corneal response to injury. Prog. Retin. Eye Res. *21*, 449–464.
16. Kenchegowda, S., and Bazan, H.E.P. (2010). Significance of lipid mediators in corneal injury and repair. J. Lipid Res. *51*, 879–891.
17. Basil, M.C., and Levy, B.D. (2016). Specialized pro-resolving mediators: endogenous regulators of infection and inflammation. Nat. Rev. Immunol. *16*, 51–67.
18. Jia, C., Zhu, W., Ren, S., Xi, H., Li, S., and Wang, Y. (2011). Comparison of genome-wide gene expression in suture- and alkali burn-induced murine corneal neovascularization. Mol. Vis. *17*, 2386–2399.
19. North, T.E., Goessling, W., Walkley, C.R., Lengerke, C., Kopani, K.R., Lord, A.M., Weber, G.J., Bowman, T.V., Jang, I.H., Grosser, T., et al. (2007). Prostaglandin E2 regulates vertebrate haematopoietic stem cell homeostasis. Nature *447*, 1007–1011.
20. Nakanishi, M., and Rosenberg, D.W. (2013). Multifaceted roles of PGE2 in inflammation and cancer. Semin. Immunopathol. *35*, 123–137.
21. Cheng, H., Huang, H., Guo, Z., Chang, Y., and Li, Z. (2021). Role of prostaglandin E2 in tissue repair and regeneration. Theranostics *11*, 8836–8854.
22. Duffin, R., O'Connor, R.A., Crittenden, S., Forster, T., Yu, C., Zheng, X., Smyth, D., Robb, C.T., Rossi, F., Skouras, C., et al. (2016). Prostaglandin E(2) constrains systemic inflammation through an innate lymphoid cell-IL-22 axis. Science *351*, 1333–1338.
23. Yao, C., Sakata, D., Esaki, Y., Li, Y., Matsuoka, T., Kuroiwa, K., Sugimoto, Y., and Narumiya, S. (2009). Prostaglandin E2-EP4 signaling promotes immune inflammation through Th1 cell differentiation and Th17 cell expansion. Nat. Med. *15*, 633–640.
24. Cilenti, F., Barbiera, G., Caronni, N., Iodice, D., Montaldo, E., Barresi, S., Lusito, E., Cuzzola, V., Vittoria, F.M., Mezzanzanica, L., et al. (2021). A PGE_2-MEF2A axis enables context-dependent control of inflammatory gene expression. Immunity *54*, 1665–1682.e14.
25. Loynes, C.A., Lee, J.A., Robertson, A.L., Steel, M.J., Ellett, F., Feng, Y., Levy, B.D., Whyte, M.K.B., and Renshaw, S.A. (2018). PGE2 production at sites of tissue injury promotes an anti-inflammatory neutrophil phenotype and determines the outcome of inflammation resolution *in vivo*. Sci. Adv. *4*, eaar8320.
26. Zhang, Y., and Daaka, Y. (2011). PGE2 promotes angiogenesis through EP4 and PKA Cgamma pathway. Blood *118*, 5355–5364.
27. Zhang, Y., Desai, A., Yang, S.Y., Bae, K.B., Antczak, M.I., Fink, S.P., Tiwari, S., Willis, J.E., Williams, N.S., Dawson, D.M., et al. (2015). TISSUE REGENERATION. Inhibition of the prostaglandin degrading enzyme 15-PGDH potentiates tissue regeneration. Science *348*, aaa2340.
28. Goessling, W., North, T.E., Loewer, S., Lord, A.M., Lee, S., Stoick-Cooper, C.L., Weidinger, G., Puder, M., Daley, G.Q., Moon, R.T., and Zon, L.I. (2009). Genetic interaction of PGE2 and Wnt signaling regulates developmental specification of stem cells and regeneration. Cell *136*, 1136–1147.
29. Miyoshi, H., VanDussen, K.L., Malvin, N.P., Ryu, S.H., Wang, Y., Sonnek, N.M., Lai, C.W., and Stappenbeck, T.S. (2017). Prostaglandin E2 promotes intestinal repair through an adaptive cellular response of the epithelium. EMBO J. *36*, 5–24.
30. Franco, F., Wenes, M., and Ho, P.C. (2018). Sparks Fly in PGE2-Modulated Macrophage Polarization. Immunity *49*, 987–989.
31. Sanin, D.E., Matsushita, M., Klein Geltink, R.I., Grzes, K.M., van Teijlingen Bakker, N., Corrado, M., Kabat, A.M., Buck, M.D., Qiu, J., Lawless, S.J., et al. (2018). Mitochondrial Membrane Potential Regulates Nuclear Gene Expression in Macrophages Exposed to Prostaglandin E2. Immunity *49*, 1021–1033.e6.
32. Nakanishi, Y., Nakatsuji, M., Seno, H., Ishizu, S., Akitake-Kawano, R., Kanda, K., Ueo, T., Komekado, H., Kawada, M., Minami, M., and Chiba, T. (2011). COX-2 inhibition alters the phenotype of tumor-associated macrophages from M2 to M1 in Apc(Min/+) mouse polyps. Carcinogenesis *32*, 1333–1339.
33. Zhu, L., Xu, C., Huo, X., Hao, H., Wan, Q., Chen, H., Zhang, X., Breyer, R.M., Huang, Y., Cao, X., et al. (2019). The cyclooxygenase-1/mPGES-1/endothelial prostaglandin EP4 receptor pathway constrains myocardial ischemia-reperfusion injury. Nat. Commun. *10*, 1888.
34. Jiang, L., He, W., Tang, F., Tang, N., Huang, G., Huang, W., Wu, X., Guan, J., Zeng, S., Li, M., et al. (2021). Epigenetic Landscape Analysis of the Long Non-Coding RNA and Messenger RNA in a Mouse Model of Corneal Alkali Burns. Invest. Ophthalmol. Vis. Sci. *62*, 28.
35. Li, Y., Soendergaard, C., Bergenheim, F.H., Aronoff, D.M., Milne, G., Riis, L.B., Seidelin, J.B., Jensen, K.B., and Nielsen, O.H. (2018). COX-2-PGE(2) Signaling Impairs Intestinal Epithelial Regeneration and Associates with TNF Inhibitor Responsiveness in Ulcerative Colitis. EBioMedicine *36*, 497–507.
36. Li, Y., Ge, L., Chen, X., Mao, Y., Gu, X., Ren, B., Zeng, Y., Chen, M., Chen, S., Liu, J., et al. (2021). The common YAP activation mediates corneal epithelial regeneration and repair with different-sized wounds. NPJ Regen. Med. *6*, 16.
37. Català, P., Groen, N., Dehnen, J.A., Soares, E., van Velthoven, A.J.H., Nuijts, R.M.M.A., Dickman, M.M., and LaPointe, V.L.S. (2021). Single cell transcriptomics reveals the heterogeneity of the human cornea to identify novel markers of the limbus and stroma. Sci. Rep. *11*, 21727.
38. Zhang, Y., Lv, X., Chen, L., and Liu, Y. (2023). The role and function of CLU in cancer biology and therapy. Clin. Exp. Med. *23*, 1375–1391.
39. Senchenkova, E.Y., Ansari, J., Becker, F., Vital, S.A., Al-Yafeai, Z., Sparkenbaugh, E.M., Pawlinski, R., Stokes, K.Y., Carroll, J.L., Dragoi, A.M., et al. (2019). Novel Role for the AnxA1-Fpr2/ALX Signaling Axis as a Key Regulator of Platelet Function to Promote Resolution of Inflammation. Circulation *140*, 319–335.
40. Feng, J., Lu, S.S., Xiao, T., Huang, W., Yi, H., Zhu, W., Fan, S., Feng, X.P., Li, J.Y., Yu, Z.Z., et al. (2020). ANXA1 Binds and Stabilizes EphA2 to Promote Nasopharyngeal Carcinoma Growth and Metastasis. Cancer Res. *80*, 4386–4398.
41. Yu, C., Chen, H., Qi, X., Chen, P., and Di, G. (2019). Annexin A1 mimetic peptide Ac2-26 attenuates mechanical injury induced corneal scarring and inflammation. Biochem. Biophys. Res. Commun. *519*, 396–401.
42. André da Silva, R., Moraes de Paiva Roda, V., Philipe de Souza Ferreira, L., Oliani, S.M., Paula Girol, A., and Gil, C.D. (2022). Annexins as potential targets in ocular diseases. Drug Discov. Today *27*, 103367.
43. Liao, W.I., Wu, S.Y., Wu, G.C., Pao, H.P., Tang, S.E., Huang, K.L., and Chu, S.J. (2017). Ac2-26, an Annexin A1 Peptide, Attenuates Ischemia-Reperfusion-Induced Acute Lung Injury. Int. J. Mol. Sci. *18*, 1771.
44. Castro-Mondragon, J.A., Riudavets-Puig, R., Rauluseviciute, I., Lemma, R.B., Turchi, L., Blanc-Mathieu, R., Lucas, J., Boddie, P., Khan, A., Manosalva Pérez, N., et al. (2022). JASPAR 2022: the 9th release of the open-access database of transcription factor binding profiles. Nucleic Acids Res. *50*, D165–D173.
45. Choudhry, M.A., Mao, H., Haque, F., Khan, M., Fazal, N., and Sayeed, M.M. (2002). Role of NFAT and AP-1 in PGE2-mediated T cell suppression in burn injury. Shock *18*, 212–216.
46. Simonson, M.S., Herman, W.H., and Dunn, M.J. (1994). PGE2 induces c-fos expression by a cAMP-independent mechanism in glomerular mesangial cells. Exp. Cell Res. *215*, 137–144.
47. Chou, J., Provot, S., and Werb, Z. (2010). GATA3 in development and cancer differentiation: cells GATA have it! J. Cell. Physiol. *222*, 42–49.
48. Wan, Y.Y. (2014). GATA3: a master of many trades in immune regulation. Trends Immunol. *35*, 233–242.
49. Khazaeli Najafabadi, M., Mirzaeian, E., Memar Montazerin, S., Tavangar, A.R., Tabary, M., and Tavangar, S.M. (2021). Role of GATA3 in tumor diagnosis: A review. Pathol. Res. Pract. *226*, 153611.
50. Saotome, M., Poduval, D.B., Nair, R., Cooper, M., and Takaku, M. (2022). GATA3 Truncation Mutants Alter EMT Related Gene Expression

via Partial Motif Recognition in Luminal Breast Cancer Cells. Front. Genet. *13*, 820532.

51. Sugimoto, Y., and Narumiya, S. (2007). Prostaglandin E receptors. J. Biol. Chem. *282*, 11613–11617.
52. Bryson, T.D., and Harding, P. (2022). Prostaglandin E2 EP receptors in cardiovascular disease: An update. Biochem. Pharmacol. *195*, 114858.
53. Wang, Z., Wei, X., Ji, C., Yu, W., Song, C., and Wang, C. (2022). PGE2 inhibits neutrophil phagocytosis through the EP2R-cAMP-PTEN pathway. Immun. Inflamm. Dis. *10*, e662.
54. An, Y., Yao, J., and Niu, X. (2021). The Signaling Pathway of PGE_2 and Its Regulatory Role in T Cell Differentiation. Mediat. Inflamm. *2021*, 9087816.
55. Ho, A.T.V., Palla, A.R., Blake, M.R., Yucel, N.D., Wang, Y.X., Magnusson, K.E.G., Holbrook, C.A., Kraft, P.E., Delp, S.L., and Blau, H.M. (2017). Prostaglandin E2 is essential for efficacious skeletal muscle stem-cell function, augmenting regeneration and strength. Proc. Natl. Acad. Sci. USA *114*, 6675–6684.
56. Zhan, P., Cui, Y., Cao, Y., Bao, X., Wu, M., Yang, Q., Yang, J., Zheng, H., Zou, J., Xie, T., et al. (2022). PGE_2 promotes macrophage recruitment and neovascularization in murine wet-type AMD models. Cell Commun. Signal. *20*, 155.
57. Toris, C.B., Gabelt, B.T., and Kaufman, P.L. (2008). Update on the mechanism of action of topical prostaglandins for intraocular pressure reduction. Surv. Ophthalmol. *53*, S107–S120.
58. Alm, A. (2014). Latanoprost in the treatment of glaucoma. Clin. Ophthalmol. *8*, 1967–1985.
59. Vecchi, L., Araujo, T.G., Azevedo, F., Mota, S.T.S., Avila, V.M.R., Ribeiro, M.A., and Goulart, L.R. (2021). Phospholipase A_2 Drives Tumorigenesis and Cancer Aggressiveness through Its Interaction with Annexin A1. Cells *10*, 1472.
60. Börgeson, E., Johnson, A.M.F., Lee, Y.S., Till, A., Syed, G.H., Ali-Shah, S.T., Guiry, P.J., Dalli, J., Colas, R.A., Serhan, C.N., et al. (2015). Lipoxin A4 Attenuates Obesity-Induced Adipose Inflammation and Associated Liver and Kidney Disease. Cell Metab. *22*, 125–137.
61. Das, U.N. (2021). Essential Fatty Acids and Their Metabolites in the Pathobiology of Inflammation and Its Resolution. Biomolecules *11*, 1873.
62. Livak, K.J., and Schmittgen, T.D. (2001). Analysis of relative gene expression data using real-time quantitative PCR and the 2(-Delta Delta C(T)) Method. Methods *25*, 402–408.
63. Stuart, T., Butler, A., Hoffman, P., Hafemeister, C., Papalexi, E., Mauck, W.M., 3rd, Hao, Y., Stoeckius, M., Smibert, P., and Satija, R. (2019). Comprehensive Integration of Single-Cell Data. Cell *177*, 1888–1902.e21.
64. Subramanian, A., Tamayo, P., Mootha, V.K., Mukherjee, S., Ebert, B.L., Gillette, M.A., Paulovich, A., Pomeroy, S.L., Golub, T.R., Lander, E.S., and Mesirov, J.P. (2005). Gene set enrichment analysis: a knowledge-based approach for interpreting genome-wide expression profiles. Proc. Natl. Acad. Sci. USA *102*, 15545–15550.
65. Hellman, L.M., and Fried, M.G. (2007). Electrophoretic mobility shift assay (EMSA) for detecting protein-nucleic acid interactions. Nat. Protoc. *2*, 1849–1861.

STAR★METHODS

KEY RESOURCES TABLE

REAGENT or RESOURCE	SOURCE	IDENTIFIER
Antibodies		
CREB1	Beyotime	Cat#AG1687
GATA3	Beyotime	Cat#AG1992
p-CREB1 (Ser133)	Beyotime	Cat#AF5785
p-GATA3 (Ser308)	Beyotime	Cat#AF1702
β-ACTIN	Beyotime	Cat#AF2811
Tubulin	Beyotime	Cat#AF2827
Horseradish Peroxidase-Conjugated IgG antibodies	Beyotime	Cat#A0208, Cat#A0216
Bacterial and virus strains		
T1 Ultracompetent Cells	Bioground	Cat#BG0008
Chemicals, peptides, and recombinant proteins		
PGE2	Cayman Chemical	Cat#14010
dmPGE2	Cayman Chemical	Cat#14750
CAY10526	Cayman Chemical	Cat#10010088
Ac2-26	Tocris Bioscience	Cat#1845
NaOH	Sangon biotech	Cat#A620617
Phosphate buffer saline (PBS)	HyClone	Cat#SH30256.LS
DMSO	Sigma-Aldrich	Cat#D8418
TRIzol reagent	Invitrogen	Cat#15596026
Fluorescein sodium	Solarbio	Cat#F8140
BSA	Sangon biotech	Cat#A602440-0050
TBE	Beyotime	Cat#ST723
Tris-buffered saline (TBS)	Beyotime	Cat#ST663
FBS	HyClone	Cat#SH30084.03
Penicillin/streptomycin	Gibco	Cat#15140122
Lipofectamine™ 2000 Reagent	Invitrogen	Cat#11668019
RIPA lysis buffer	Beyotime	Cat#P0013B
DMEM with high glucose	Gibco	Cat#11965092
Critical commercial assays		
Nuclear and Cytoplasmic Protein Extraction Kit	Beyotime	Cat#P0028
Dual-Lumi™ II Luciferase Assay Kit	Beyotime	Cat#RG089M
FastKing gDNA Dispelling RT SuperMix kit	TIANGEN	Cat# KR116
SYBR Prime qPCR Set	Baoguang Biotechnology	Cat#BG0014
SDS-PAGE protein loading buffer	Beyotime	Cat#P0015
Proteases and phosphatases inhibitors	Beyotime	Cat#P1050
Enhanced chemiluminescence detection reagents	Solarbio	Cat#PE0010
Deposited data		
RNA-seq data of corneas after alkali burns	SRA database	SRR13449163, SRR13449162, SRR13449161, SRR13449160, SRR13449159, SRR13449158
RNA-seq data of 16 hours after corneal injury	BioProject database	PRJNA669218

(*Continued on next page*)

Continued

REAGENT or RESOURCE	SOURCE	IDENTIFIER
Single-cell transcriptome data of the corneas	GEO database	GSE186433
RNA-seq data of intestinal organoids treated with PGE2	GEO database	GSE116936
RNA-seq data of GATA3 vector overexpresion cells	GEO database	GSE216413
RNA-seq data of GATA3 mutant cells	GEO database	GSE190381
Experimental models: Cell lines		
Human corneal epithelial cells (hCECs)	BeNa Cuture Collection	Cat#BNCC337876
Experimental models: Organisms/strains		
C57BL/6 mice	Third Military Medical University	N/A
Oligonucleotides		
Primers, see Table S5	This paper	N/A
Recombinant DNA		
pGL4.10 vector	Promega	N/A
pcDNA3.1(+) expression vector	Invitrogen	Cat#V790-20
pcDNA3.1(+)-ANXA1	This paper	N/A
pcDNA3.1(+)-GATA3	This paper	N/A
pGL4.10-*ANXA1* Promoter-Luc (with different length: 500 bp, 600 bp, 700 bp, 800 bp, 900 bp, 1000 bp, 1500 bp, 2000 bp)	This paper	N/A
pGL4.10-*1000-GATA3 CRE1* mut -Luc	This paper	N/A
pGL4.10-*1000-GATA3 CRE2* mut -Luc	This paper	N/A
pGL4.10-*1000-CREB1*mut -Luc	This paper	N/A
pGL4.10-*1000-GATA3 CRE2* mut +*CREB1*mut -Luc	This paper	N/A
Software and algorithms		
ImageJ	https://imagej.net/ij/	N/A
GraphPad Prism	Dotmatics	version 8.0
R	https://www.r-project.org/	version 3.5.2

RESOURCE AVAILABILITY

Lead contact

Further information and requests for resources and reagents should be directed to and will be fulfilled by the lead contact, Yong Liu (liuyy99@163.com).

Materials availability

This study does not generate new unique reagents.

Data and code availability

- This paper analyzes existing, publicly available data. These accession numbers for the datasets have been listed in the text and the key resources table.
- This paper does not report original code.
- Any additional information required to reanalyze the data reported in this paper is available from the lead contact upon request.

EXPERIMENTAL MODEL AND STUDY PARTICIPANT DETAILS

Cell lines

Human corneal epithelial cells (hCECs) were obtained from BeNa Cuture Collection and stored in the eye bank of Southwest Hospital, Third Military Medical University (Army Medical University). HCECs were cultured at 37°C in Dulbecco's Modified Eagle Medium (DMEM) with high glucose (Gibco) supplemented with 10% (v/v) FBS (Hyclone) and 1% (v/v) penicillin/streptomycin (Gibco) in a humidified 5% CO2 incubator.

In vivo mouse studies

Male C57BL/6J mice (8-week-old) were obtained from the Third Military Medical University and housed under the standard ambient temperature and humidity with a 12-h light/12-h dark cycle. The study was conducted with the approval of the Committee of Animal Care of the Third Military Medical University (AMUWEC20223993) and all the animal experimental procedures were carried out following the ARVO Statement for the Use of Animals in Ophthalmic and Vision Research. Male littermates were randomly assigned to experimental groups.

Plasmids

The pcDNA3.1(+) expression vector was purchased from Invitrogen (CA, USA) and stored in our laboratory. It was used to construct the overexpression vectors for *ANXA1* and *GATA3*. The pGL4.10 vector was purchased from Promega (WI, USA) to construct the dual luciferase reporter vector.

Bacterial strains

The T1 Ultracompetent Cells was purchased from Baoguang Biotechnology (Chongqing, CHN) and used as the competent cells to construct the vectors.

Chemical reagents

PGE2 was purchased from Cayman Chemical Company (MI, USA) and dissolved in DMSO to make a 10 mg/mL stock solution that was further diluted to different final concentrations for experiments. DmPGE2 was purchased from Cayman Chemical Company with solution in methyl acetate and the solvent was replaced with phosphate buffer saline (PBS, HyClone) and diluted to different final concentrations by blowing dry with a nitrogen blowing instrument before use. CAY10526 (short for10526), a specific inhibitor for PTGES, was purchased from Cayman Chemical Company and dissolved in DMSO to make a 10 mg/mL stock solution that was further diluted to 10 μM for experiments. ANXA1 mimetic peptide Ac2-26 was purchased from Tocris Bioscience Company (Bristol, UK) and dissolved in PBS to make a 10 ng/μL concentration. Fluorescein sodium was purchased from Solarbio Company (Beijing, CHN) and dissolved in PBS to a 10 mg/mL concentration. NaOH was purchased from Sangon biotech Company (Shanghai, CHN) and dissolved in sterile water to a 0.2 M concentration before experiment.

METHOD DETAILS

Alkali-induced corneal injury

Male C57BL/6J mice were intraperitoneally injected with 1% sodium pentobarbital at 25 mg/kg body weight, and dropped with the ocular surface anesthesia. The filter paper with 2 mm-diameter treated with 0.2 M NaOH was gently placed on the cornea of the mouse for 30 s, then immediately removed the filter paper and washed the eyes with more than 20 mL PBS and wiped off excess PBS with absorbent paper.

Fluorescein sodium staining

5 μL fluorescein sodium with a 10 mg/mL concentration was dropped into the ocular surface for 10 s, then the eyes were washed with PBS until no fluorescein sodium solution residue. We absorbed the excess fluid with cotton paper and photographed it with a camera (Nikon D5500). The wound closure was calculated by the initial relative fluorescein sodium positive reaction area minus termination relative area and divided by the initial relative fluorescein sodium positive reaction area and multiplied by 100%.[36]

Drug's treatment

PGE2 and dmPGE2 were used to increase the content of PGE2 in cells and mice. PGE2 was dissolved in DMSO to make a 10 mg/mL stock solution and further diluted to different final concentrations with distillation-distillation H2O (ddH2O). 0.1% DMSO was used as the DMSO vehicle control for PGE2. DmPGE2 was replaced with phosphate buffer saline (PBS, HyClone) and diluted to different final concentrations with PBS. PBS was used as the PBS vehicle control for dmPGE2. All mice were treated with local ocular administration for 4 consecutive days. 100 nM, 10 μM, and 250 μM PGE2 and dmPGE2 with 5 μL were dropped into the corneas of the mice three times a day. And 5 μL 10 ng/μL ANXA1 mimetic peptide Ac2-26 was also used to treat the corneas after alkali burns. The PBS vehicle was used as the control group. The final concentration of PGE2 and dmPGE2 treatment is 1 nM, 10 nM, 100 nM, 1μM, 10 μM, 25 μM, and 50 μM respectively in hCECs. 10526 was used to inhibit the PGE2 synthesis in hCECs with 10 μM work concentration and 0.1% DMSO was used as the DMSO vehicle control.

RNA extraction and quantitative real time PCR (qPCR)

The collected mice corneas and hCECs were suspended in TRIzol reagent (Takara, Osaka, Japan) to extract total RNA. 1 μg total RNA was used to synthesize cDNA with a FastKing gDNA Dispelling RT SuperMix kit (TIANGEN, Beijing, CHN). qPCR was conducted using SYBR Prime qPCR Set (Baoguang Biotechnology, Chongqing, CHN) on CFX96 RT-PCR System (Bio-Rad, Hercules, CA, USA) according to the manufacturer's instructions. The gene expression was normalized to the housekeeping gene (*GAPDH*) and analyzed using the $2^{-\Delta\Delta CT}$ method.[62] qPCR primers sequence used in this study were listed in Table S5.

Single-cell RNA-seq and bulk RNA-seq analysis

Single-cell transcriptome data with GEO database: GSE186433 [37] was used to analyze the expression and distribution of co-expressed differential genes in corneas. And the analysis was performed as previously described[63] and implemented using R version 3.5.2 and the package Seurat version 2.3.4. The RNA-seq data on 7 days after alkali-induced corneal injury in NCBI Sequence Read Archive (SRA) database: SRR13449163, SRR13449162, SRR13449161, SRR13449160, SRR13449159, and SRR13449158[34] was downloaded using sratoolkit (v3.0.1). Then the data was transformed and analyzed as previously described.[34] In briefly, these sra files were converted into fastq files by fastq-dump, and MD5 detection was performed to ensure the integrity for the downstream analysis. We checked the data quality by fastqc and perform the fastq file data quality control by fastp and trim-galore software. The reference genome index was directly downloaded from https://cloud.biohpc.swmed.edu/index.php/s/grcm38/download. Then, the clean data was aligned to the reference genome using hisat2 (v2.2.1) to generate a sam file. And the sam file was convert into the bam file by samtools (v1.16). Finally, we use the featurecount in subread to count the number of reads for each gene. DESeq2 (v1.36.0) was employed to detect the differentially expressed genes (DEGs). GSEA was performed in the GSEA (v.4.0) software available at https://software.broadinstitute.org/gsea.[64] The RNA-seq data for 16 hours after corneal injury in NCBI Sequence Read Archive (SRA) under the BioProject accession number PRJNA 669218[36] was used to analyze. The transcriptome data of intestinal organoids treated with 1 μM PGE2 download from the GEO database: GSE116936 [35] was also used to analyze the upregulated genes induced by PGE2. The transcriptome data in the GEO database: GSE216413, GSE190381 [50] were used to analyze *ANXA1* expression after the changes of GATA3.

In vitro scratch wound healing assay

HCECs were cultured and inoculated into 6-well culture plates at a final 1×10^6 cells/well density. A straight gap was scratched with a 200 μL micropipette tip in the monolayer cells after the confluence reached 100%, and the cellular debris was washed with PBS. The hCECs were treated with different dosages of PGE2, dmPGE2, 10526, and vehicle (0.1% DMSO; or PBS), then incubated for 36 hours under indicated conditions. The wound area was measured under a light microscope (×40) at different time points (0, 12, 24, and 36 h) and analyzed using Image J. The wound closure was calculated as the percentage of the healed epithelial area at each time point/initial scratch area.

Vector constructions

The sequences of *ANXA1* and *GATA3* coding regions were obtained from GeneBank: NM_000700.3 and NM_001002295.2, respectively. The primers were designed using primer 5.0 software and synthesized by the Beijing Genomics Institution (Beijing, CHN). The open reading frames of *ANXA1* and *GATA3* were amplified from the cDNA of the hCECs and cloned into the pcDNA3.1(+) expression vector with *Nhe*I and *Bam*HI. The primers for expression vector construction are given in Table S5.

The 2000 bp upstream regulatory sequence of the *ANXA1* promoter was amplified from the genome of hCECs and truncated to different fragment lengths. The promoters with different lengths were ligated to the pGL4.10 vector with the restriction enzymes *Xho*I and *Hin*dIII. To analyze specific cis-elements in the *ANXA1* promoter, the 2000 bp promoter of *ANXA1* were predicted in JASPAR database (https://jaspar.genereg.net).[44] To analyze the effects of GATA3 and CREB1 on *ANXA1* promoter activity, the mutation vectors of pGL4.10-1000 Luc with disruption of the GATA3 and CREB1 CRE were constructed by site-specific mutagenesis. The mutation sequences were amplified using a unique primer containing the mutated GATA3 CRE or CREB1 CRE. The core sites of GATA3 CRE, i.e., "ATATCT" and "AGATAG", were changed to "GCGCTC" and "GAGCGA", respectively. The CREB1 CRE sequence "TGATGTCA" was changed to "CAGCACTG". And the mutation reporter vectors of GATA3 CRE2 and CREB1 CRE co-mutation was also constructed to analyze. The primers for the vector construction are listed in Table S5.

Western blot

The hCECs were collected in PBS and pelleted by centrifugation at 300 g for 5 min. Then the cells were lysed in a RIPA lysis buffer (Beyotime Biotechnology, Shanghai, CHN) mixture with proteases and phosphatases inhibitors (Beyotime Biotechnology). Samples were incubated on ice for 30 min and centrifugated at 15,000 g for 10 min. The supernatants were the protein lysates. The protein lysates were mixed with SDS-PAGE protein loading buffer (Beyotime Biotechnology) and denatured at 100°C for 10 min. Then the samples were separated by SDS-polyacrylamide gel electrophoresis under reducing conditions and transferred to a PVDF membrane. The membranes were blocked in 5% BSA in tris-buffered saline (TBS; Beyotime Biotechnology) and 0.1% Tween 20 (TBST) for 1 h at room temperature. The membranes were incubated with primary antibodies at 1:1000 dilution overnight at 4°C. Then the membranes were incubated with peroxidase-conjugated secondary antibodies (anti-rabbit or anti-mouse) at a 1:10,000 dilution for 1 h at room temperature after being washed three times with TBST. The membranes were washed three times with TBST and incubated with Enhanced chemiluminescence detection reagents (Beyotime Biotechnology). ChemiDoc MP imaging system (Bio-rad) was used to detect the chemiluminescence of stripes. The results were analyzed using Image Lab software with β-actin or α-tubulin as a loading control. The original unedited blots used in the paper are provided in Figures S5–S7.

Dual luciferase reporter assay

HCECs were inoculated into 24-well culture plates in a monolayer cell with 80% confluence. The constructed vectors for the *ANXA1* promoter were transfected into hCECs by Lipofectamine™ 2000 Reagent (Invitrogen, CA, USA). Total 1 μg vectors was transfected into one well of 24-well culture plates. The ratio (w/w) of the reporter vector with the *ANXA1* promoter to control reporter vector PRL-CMV was 1:0.1. The ratio

(w/w) of the reporter vector with the *ANXA1* promoter to pcDNA3.1(+)-GATA3 was 1:1. After culturing for 7 h, the transfection mixture was replaced with 500 μL fresh medium. The cells were cultured further for 36 or 48 h and then harvested for luciferase activity assays. Luciferase activity was measured using Dual-Lumi™ II Luciferase Assay Kit (Beyotime Biotechnology) according to the manufacturer's instructions. The cells were washed three times with PBS, then added with 150 μL lysis buffer to each well. Samples were incubated for 10 min at room temperature and centrifugated at 12,000 g for 5 min. The 100 μL supernatants were transferred to a black 96-well microplate and incubated with 100 μL Dual-Lumi™ II firefly luciferase detection reagent for 10 min, then chemiluminescence detection was performed using a multifunctional microplate reader. Finally, added 100 μL Dual-Lumi™ II renilla luciferase detection reagent and incubated for 10 min, and detected the renilla luciferase by the multifunctional microplate reader. The relative luciferase was calculated by firefly luciferase divided by renilla luciferase.

Electrophoretic mobility-shift assay (EMSA)

To analyze whether GATA3 and CREB1 could bind to the putative CRE in the *ANXA1* promoter, EMSAs were used, as previously described.[65] The probes were labeled with biotin at the 5'terminus (synthesized by Sangon Biotech). Nuclear proteins were extracted using a Nuclear and Cytoplasmic Protein Extraction Kit (Beyotime Biotechnology). EMSAs were carried out according to the manufacturer's instructions (EMSA/Gel-Shift Kit; Beyotime Biotechnology). The probes were incubated with nuclear proteins at room temperature for 30 min. Then the DNA-protein binding reaction mixtures were loaded onto 5% (w/v) native polyacrylamide gels and electrophoresed in 0.5×TBE (Beyotime Biotechnology). After electrophoresis, the protein/nucleic acid complexes were transferred to a nylon membrane (Roche, Indianapolis, IN, USA). And the membrane was cross-linked immediately on the UV cross-linking instrument with 120 mJ/cm^2 for 40 s. 16 mL blocking buffer was added to the membrane and shaken slowly for 15 min after cross-linking. Abandon the blocking buffer, add biotin antibody diluted in blocking buffer with 1: 2000 ratio and shake slowly for 1 h. The membrane was transferred to a new container and balanced with 30 mL of equilibrium buffer for 5 min after washed with washing buffer for 3 times. Then the membrane was detected using an enhanced chemiluminescence system with a ChemiDoc MP imaging system.

QUANTIFICATION AND STATISTICAL ANALYSIS

All experiments were repeated more than three times independently, and all data were analyzed using GraphPad Prism software. Data were presented as arithmetic means with error bars, which reflect the standard error of the mean (SEM) as indicated. Statistical significance was determined using the unpaired t test when comparing two groups, and *$p < 0.05$, **$p < 0.01$, ***$p<0.001$, ****$p < 0.0001$, ns, no significance.